

On electronic shells surrounding charged insulated metallic clusters

K. Dietrich and M. Garny

Physikdepartment of the Technische Universität München

D-85747 Garching (FRG)

K. Pomorski

Katedra Fizyki Teoretycznej, Uniwersytet Marii Curie-Skłodowskiej

PL-20031 Lublin (Poland)

November 21, 2018

Abstract

We determine the wavefunctions of electrons bound to a positively charged mesoscopic metallic cluster covered by an insulating surface layer. The radius of the metal core and the thickness of the insulating surface layer are of the order of a couple of ångström. We study in particular the electromagnetic decay of externally located electrons into unoccupied internally located states which exhibits a resonance behaviour. This resonance structure has the consequence that the lifetime of the “mesoscopic atoms” may vary by up to 6 orders of magnitude depending on the values of the parameters (from sec to years).

1 Introduction

Clusters consisting of some 10^2 to 10^5 atoms, which can be produced for instance in the course of the condensation of vapour, have attracted great interest during the last 20 years. These “mesoscopic” clusters were found to exhibit classical as well as quantum mechanical features. In the special case of metallic clusters [1], the conduction electrons, which move in the average potential produced by the positively charged ions, exhibit shell effects. As a consequence, the binding energy of the cluster becomes a function of the number of free electrons (and thus also of the number of ions). In turn, this implies measurable variations of the formation probability of a cluster as a function of its mass in a thermal vapour-gas equilibrium.

Other interesting types of mesoscopic systems are the so-called “fullerenes” which represent a crystal of atoms covering a closed, usually spherical surface [2]. A number of review articles exist on this exciting new field of physics (see for instance Ref. [3] and Ref. [4] and books mentioned at the end of Ref. [1] and Ref. [2]).

In the present paper, we consider a mesoscopic system which consists of a spherical metallic core of radius R_2 carrying Z positive charges and surrounded by an insulating layer of external radius R_1 (see Fig. 1). We determine analytically the bound states of a single electron in the potential $V(r)$ which is produced by the positive surface charge density of the metallic core and the insulating dielectric surface layer. As in the case of an ordinary atom, these

single electron wave functions describe also approximately the case that several electrons are bound in this potential. For Z bound electrons, the system has total charge 0. Because of the obvious similarity of this system with an atom or ion, we refer to it as a "mesoscopic atom" or "mesoscopic ion".

As one can surmise, there are two different types of bound electronic states: electrons localized in the metallic core inside of the insulating layer (region II, Fig. 1) and electrons localized in the vacuum outside of the insulating layer (region 0, Fig. 1). The bound states localized outside are reminiscent of the bound states of an electron in the Coulomb potential of the atomic nucleus. We are mainly interested in these externally localized electronic states ("class 1-states") and their decay into lower-lying bound states predominantly localized within the metallic core ("class 2-states").

The paper is organized as follows:

In Sec. 2, we formulate the single-particle Hamiltonian and determine the eigenfunctions and eigenenergies of bound electrons. In doing so, we take into account the polarization of the insulating surface layer which is produced by the uniform positive charge distribution on the surface S_2 of the metal, but we neglect the additional polarization effects produced by the externally localized electrons.

In Sec. 3 we determine these additional polarization effects within the classical Maxwellian electrodynamics. They lead to an additional potential acting on the electrons which is of importance close to the surface S_1 of the insulator. So far, we have not yet studied the effect of this additional potential on the externally localized electrons.

The Sec. 4 is dedicated to a presentation of the results. In Subsec. 4.1, we describe the procedure which we used in order to obtain the eigenvalues and eigenfunctions and we present typical examples of spectra and wavefunctions. In Subsec. 4.2, we discuss the electromagnetic decay of a predominantly externally localized bound electron into a lower-lying internally localized state. We show that the transition rate and the corresponding life-time may vary by several orders of magnitude depending on the parameters of the system.

In general, the transition is hindered by the small overlap between externally and internally localized states ("class 1-states" and "class 2-states") if the insulating surface layer is sufficiently thick. In particular, we discuss the special role in this decay of "class 3-states" which exhibit non-negligible amplitudes both in the external region 0 and the internal region II.

Finally, in Sec. 5, we summarize the results and discuss some related open questions.

2 Theory

In the single-particle Hamiltonian for an electron bound to a positively charged and insulated metallic core (M = mass of the electron)

$$\widehat{H} = \widehat{T} + \widehat{V} = -\frac{\hbar^2}{2M}\Delta + V(r) , \quad (1)$$

the potential $V(r)$ contains the interaction of the electron with the positive surplus charge Ze_0 (e_0 = elementary charge) and with the ionic background ("jellium") of the metal. Furthermore, it contains the effects of the insulating surface layer. The radius R_2 of the metal and the thickness ($R_1 - R_2$) of the surface layer are assumed to be of the order of 5 to 20 Å (1 Å = 10^{-10} m) and the number Z of positive charges of the metal is considered to be 1 to 5. For these dimensions of the system we may expect that, on the one hand, the dynamics of the

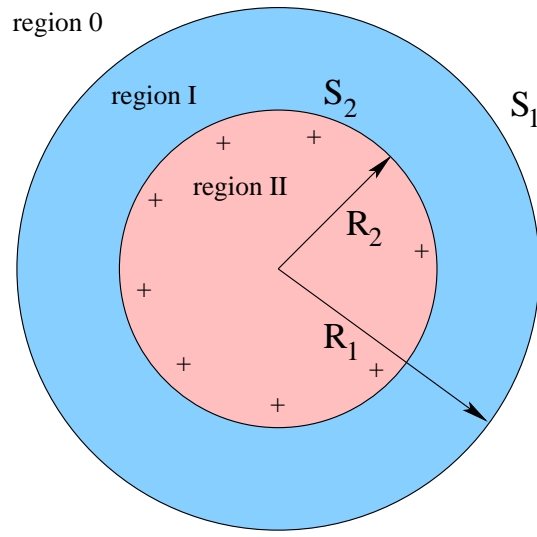


Figure 1: Schematic view of the charged metallic cluster (radius R_2 , surface S_2) covered by an insulating layer (outer radius R_1 , surface S_1). States of bound electrons predominantly localized in the surrounding vacuum ($R > R_1$, region 0) are called "class 1-states" in distinction from states localized in the metallic core ("class 2-states").

electron is fully quantum-mechanical and, on the other hand, we may use macroscopic concepts in formulating the potential $V(r)$, at least as a first approximation. So we assume that the positive surplus charge is uniformly distributed over the surface S_2 of the metal

$$\rho_2(r) = \rho_{S_2} \cdot \delta(r - R_2) = \frac{Ze_0}{4\pi R_2^2} \delta(r - R_2). \quad (2)$$

The Coulomb potential produced by this simple charge distribution acting upon an electron (charge $-e_0$) is given by

$$-e_0 \int d^3r' \frac{\rho_2(r')}{|\vec{r} - \vec{r}'|} = -\frac{Ze_0^2}{R_2} \theta_0(R_2 - r) - \frac{Ze_0^2}{r} \theta_0(r - R_2), \quad (3)$$

where $\theta_0(x)$ is the Heaviside function

$$\theta_0(x) = \begin{cases} 1 & \text{for } x > 0 \\ 0 & \text{for } x < 0 \end{cases}.$$

Inside of the metal, the conduction electrons feel not only the constant potential produced by the positive surface charge but also the attractive interaction with the ionic background which we represent by a constant negative potential $-V_{\text{II}}^0$ ($V_{\text{II}}^0 > 0$).

On the other hand, the average energy gap above the Fermi level in the insulator may act upon the electron like a repulsive barrier of a height $B_0 > 0$.

Last not least, there are polarization effects produced by the positive surplus charge and also by the charge distribution $\rho_e(\vec{r})$ of the externally (i.e. predominantly in region 0) localized electrons. The polarization effects are investigated in Sec. 3 on the basis of Maxwell's equations for the electric field \vec{E} and for the displacement field \vec{D} in the presence of homogeneous dielectric media. In the case that we only take into account the polarization effects produced by the

positive surplus charge (2), the following modifications of the Coulomb potential (3) are to be considered: Within region I, i.e. within the insulating layer, the Coulomb potential $-Ze_0^2/r$ is to be replaced by

$$-\frac{Ze_0^2}{r} \rightarrow -\frac{Ze_0^2}{r \cdot \varepsilon_I} - \frac{Ze_0^2 \cdot (\varepsilon_I - 1)}{R_1 \cdot \varepsilon_I}$$

and within region II, i.e. within the metallic core, the constant potential $-Ze_0^2/R_2$ is to be supplanted by

$$-\frac{Ze_0^2}{R_2} \rightarrow -\frac{Ze_0^2}{R_2 \varepsilon_I} - \frac{Ze_0^2 \cdot (\varepsilon_I - 1)}{R_1 \varepsilon_I} = -\frac{Ze_0^2}{R_2} + Ze_0^2 \left(\frac{1}{R_2} - \frac{1}{R_1} \right) \left(\frac{\varepsilon_I - 1}{\varepsilon_I} \right).$$

Within region 0, i.e. in the vacuum surrounding the insulating layer, the value $-Ze_0^2/r$ of the Coulomb potential (3) is unchanged.

One should note that the potential in region I assumes the value $-Ze_0^2/R_1$ at the outer surface $r = R_1$ of the insulating layer.

Let us denote the sum of the constant parts of the potentials in region I and II by

$$B := B_0 - \frac{Ze_0^2}{\varepsilon_I R_1} (\varepsilon_I - 1) \quad (4)$$

and

$$V_{\text{II}} := V_{\text{II}}^0 - Ze_0^2 \left(\frac{1}{R_2} - \frac{1}{R_1} \right) \left(\frac{\varepsilon_I - 1}{\varepsilon_I} \right). \quad (5)$$

If Z is equal to 1 or 2 and the dielectric constant ε_I exceeds 1 only slightly, and if the radii are in the range of values treated in Sec. 4, the 2nd terms on the right-hand sides of Eqs. (4) and (5) are much smaller than the 1st terms. So far, it is only these cases which we treated numerically.

Altogether, the potential $V(r)$ felt by the electron has the form

$$V(r) = - \left[V_{\text{II}} + \frac{Ze_0^2}{R_2} \right] \theta_0(R_2 - r) + \left[B - \frac{Ze_0^2}{\varepsilon_I r} \right] \theta_0(R_1 - r) \theta_0(r - R_2) - \frac{Ze_0^2}{r} \theta_0(r - R_1). \quad (6)$$

The constants V_{II} , ε_I and B_0 are empirical parameters. The potential $V(r)$ is shown in Fig. 2 for a specific choice of the parameters.

The eigenfunctions $\psi(r, \vartheta, \varphi)$ of the Schrödinger equation

$$-\frac{\hbar^2}{2M} \Delta \psi + V(r) \psi = E \psi \quad (7)$$

separate

$$\psi(r, \vartheta, \varphi) = R(r) Y_{lm}(\vartheta, \varphi) = \frac{u(r)}{r} Y_{lm}(\vartheta, \varphi) \quad (8)$$

and the radial functions $R(r)$ and $u(r)$ have to satisfy the differential equations

$$-\frac{\hbar^2}{2M} \left(\frac{d^2}{dr^2} + \frac{2}{r} \frac{d}{dr} - \frac{l(l+1)}{r^2} \right) R + V(r) R = ER, \quad (9)$$

$$-\frac{\hbar^2}{2M} \left(\frac{d^2}{dr^2} - \frac{l(l+1)}{r^2} \right) u + V(r) u = Eu, \quad (10)$$

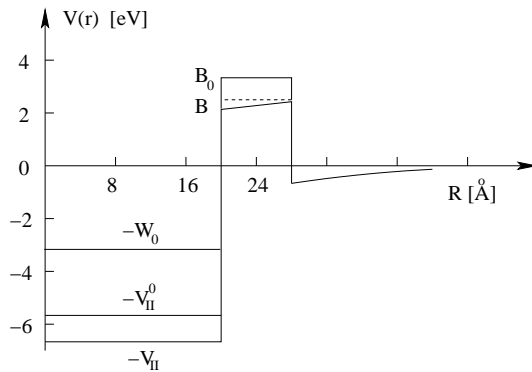


Figure 2: Semi-quantitative picture of the potential $V(r)$ for the following choice of parameters: $R_2 = 20 \text{ \AA}$; $R_1 = 30 \text{ \AA}$; $Z = 1$; $W_0 = 3.3 \text{ eV}$; $V_{\text{II}} = 6.3 \text{ eV}$; $B = 3 \text{ eV}$; $\varepsilon_{\text{I}} = 3$; $Ze_0^2/(\varepsilon_{\text{I}} \cdot R_2) = 0.24 \text{ eV}$; $Ze_0^2/(\varepsilon_{\text{I}} \cdot R_1) = 0.16 \text{ eV}$; $Ze_0^2/R_1 = 0.48 \text{ eV}$.

respectively.

For $r < R_2$ (region II), the potential $V(r)$ is constant and thus the Eq. (9) represents the differential equation for "spherical Bessel functions". Of the 2 linearly independent solutions, only the regular one, j_l , qualifies as a physical solution. Up to a normalization factor which will be determined later on, the radial function $R(r)$ in region II is simply given by

$$R_{\text{II}}(r) = j_l(\kappa_{\text{II}}r) , \quad (11)$$

where κ_{II} is defined by

$$\kappa_{\text{II}} = \sqrt{\frac{2M}{\hbar^2} \left(\frac{Ze_0^2}{R_2} + V_{\text{II}} - |E| \right)} \quad (12)$$

and $j_l(x)$ is the spherical Bessel function of the 1st kind (see Chapt. 9 of Ref. [5]). As bound states have an energy between the well depth $-(V_{\text{II}} + Ze_0^2/R_2)$ and 0, the parameter κ_{II} is assured to be real.

For $R_2 < r < R_1$ (region I) let us postpone the treatment of the general case and first turn to the simpler situation when the r -dependent term $Ze_0^2/(\varepsilon_{\text{I}}r)$ is negligible in comparison to the constant B in the entire region I. This is so, if the inequality

$$\frac{Ze_0^2}{\varepsilon_{\text{I}}R_2} \ll B \quad (13)$$

holds. For the case shown in Fig. 2, the condition is fulfilled. Generally speaking, the barrier heights B_0 range from 2 to 5 eV, and the dielectric constant ε_{I} may have values between slightly more than 1 up to more than 100 (Examples: ε_{I} (caoutchouc) = 4; ε_{I} (TiO₂-crystal) = 115).

Let us now investigate the case that the potential (6) can be approximated by

$$V(r) \approx - \left[V_{\text{II}} + \frac{Ze_0^2}{R_2} \right] \theta_0(R_2 - r) + B\theta_0(R_1 - r)\theta_0(r - R_2) - \frac{Ze_0^2}{r}\theta_0(r - R_1) . \quad (14)$$

The radial Schrödinger equation (9) in region I then assumes again the form of Bessel's differential equation. But as the energy E is lower than the barrier height B , the solution in region I is given by a linear combination of two independent "modified spherical Bessel functions" (see Chapt. 10.2 of Ref. [5]).

We choose the pair $\left\{(-i)^l j_l(iy), -\frac{\pi}{2} i^l h_l^{(1)}(iy)\right\}$, where $j_l(iy)$ and $h_l^{(1)}(iy)$ are the spherical Bessel-function and spherical Hankel-function of the 1st kind, resp., with imaginary arguments. The dimensionless real variable y is related to the radial coordinate r by

$$y = \kappa_I r , \quad (15)$$

$$\kappa_I = \sqrt{\frac{2M}{\hbar^2}(B + |E|)} . \quad (16)$$

The two factors $(-i)^l$ and $-\frac{\pi}{2} i^l$ are chosen so that the pair of solutions are simply related to the modified Bessel function of integer order $I_{l+\frac{1}{2}}(y)$ and $K_{l+\frac{1}{2}}(y)$ for which a number of rapidly converging series expansions exist (see Ref. [5], Chapt. 10.2)

$$\left\{(-i)^l j_l(iy), -\frac{\pi}{2} i^l h_l^{(1)}(iy)\right\} = \left\{\sqrt{\frac{\pi}{2y}} I_{l+\frac{1}{2}}(y), \sqrt{\frac{\pi}{2y}} K_{l+\frac{1}{2}}(y)\right\} . \quad (17)$$

The radial function $R(r)$ in region I thus has the general form

$$R_I(r) = A_I \sqrt{\frac{\pi}{2\kappa_I r}} I_{l+\frac{1}{2}}(\kappa_I r) + B_I \sqrt{\frac{\pi}{2\kappa_I r}} K_{l+\frac{1}{2}}(\kappa_I r) . \quad (18)$$

For $r > R_1$ (region 0), it is more convenient to deal with the differential Eq. (10) for $u(r)$ which has the form

$$-\frac{\hbar^2}{2M} u''(r) + \frac{\hbar^2 l(l+1)}{2Mr^2} u - \frac{Ze_0^2}{r} u = Eu . \quad (19)$$

We have to find a normalizable solution of (19). It turns out that the only normalizable solution of (19) has the form

$$u(r) = C_0 z_0^{l+1} U(a_0, b_0, z_0) e^{-\frac{z_0}{2}} , \quad (20)$$

where the dimensionless variable z_0 is related to r by

$$z_0 = 2\lambda r \quad (21)$$

with

$$\lambda = \sqrt{\frac{2M|E|}{\hbar^2}} \quad (22)$$

and where $w = U(a_0, b_0, z_0)$ is a particular solution Kummer's differential equation

$$z_0 \frac{d^2 w}{dz_0^2} + (b_0 - z_0) \frac{dw}{dz_0} - a_0 w = 0 . \quad (23)$$

The parameters a_0 and b_0 in (23) are related to the parameters in Eq. (19) by

$$a_0 = \frac{2(l+1) - d_0}{2} \quad (24)$$

$$b_0 = 2(l+1) \quad (25)$$

$$d_0 = \frac{Ze_0^2}{\hbar} \sqrt{\frac{2M}{|E|}} \quad (26)$$

and the solution $U(a_0, b_0, z_0)$ of (23) is defined as follows:

We write b_0 in the form

$$b_0 = 1 + n , \quad (27)$$

which implies

$$n = 2l + 1 . \quad (28)$$

Then the function $U(a_0, 1 + n, z_0)$, where $n = 1, \dots$ reads (see Ref. [5], Eq. (13.1.6) or Ref. [6], Eq. (13) of Chapt. 6.7.1)

$$\begin{aligned} U(a_0, n + 1, z_0) &= \frac{(-1)^{n-1}}{n! \Gamma(a_0 - n)} \cdot \left\{ M(a_0, n + 1, z_0) \ln z_0 + \right. \\ &+ \left. \sum_{\nu=0}^{\infty} \frac{(a_0)_\nu z_0^\nu}{(n+1)_\nu \nu!} [\psi(a_0 + \nu) - \psi(1 + \nu) - \psi(1 + n + \nu)] \right\} \\ &+ \frac{(n-1)!}{\Gamma(a_0)} \sum_{\nu=0}^{n-1} \frac{(a_0 - n)_\nu}{(1-n)_\nu} \cdot \frac{z_0^{\nu-n}}{\nu!} \end{aligned} \quad (29)$$

In (29), the function $\psi(x)$ is the logarithmic derivative of the Γ -function

$$\psi(x) := \frac{d\Gamma(x)}{dx} / \Gamma(x) = \frac{d \ln \Gamma(x)}{dx} \quad (30)$$

and $(c)_\nu$ is Pochhammer's symbol

$$(c)_\nu := c(c+1) \dots (c+\nu-1) = \frac{\Gamma(c+\nu)}{\Gamma(c)} . \quad (31)$$

Furthermore, $M(a_0, b_0, z_0)$ is the confluent hypergeometric function

$$M(a_0, b_0, z_0) = \sum_{\nu=0}^{\infty} \frac{\Gamma(a_0 + \nu) \Gamma(b_0)}{\Gamma(a_0) \Gamma(b_0 + \nu)} \cdot \frac{z_0^\nu}{\nu!} . \quad (32)$$

We note in passing that the complicated form of the solution (29) is due to the fact that the parameter b_0 in $U(a_0, b_0, z_0)$ is an integer. For non-integer b_0 , the function $U(a_0, b_0, z_0)$ depends in a simple way on two confluent hypergeometric functions (see Ref. [5], Eq. (13.1.3)). This form of $U(a_0, b_0, z_0)$ becomes singular if b_0 tends to an integer value. The limiting process which leads to the form (29) is discussed in Ref. [6].

For any value of b_0 , the asymptotic behaviour of U for $\Re(z_0) \rightarrow \infty$ is given by

$$U(a_0, b_0, z_0) \rightarrow \frac{1}{z_0^{a_0}} \left[1 + 0 \left(\frac{1}{|z_0|} \right) \right] \quad (33)$$

(see Ref. [5], Eq. (13.1.8)). From (33) and (20) it is clear that $u(r)$ is a normalizable function irrespectively of the value of the energy E . However, it turns out that the continuity conditions can only be met for certain discrete values of E . The radial function $R_0(r)$ in region 0 is thus defined by

$$R_0(r) = \frac{u(r)}{2\lambda r} = C_0 (2\lambda r)^l U(a_0, 2l + 2, 2\lambda r) e^{-\lambda r} . \quad (34)$$

Before we proceed to the explicit formulation of the continuity conditions, we return to the form of the solution in region I in the general case that the r -dependent term $Ze_0^2/(\varepsilon_1 r)$ is not neglected. Then the differential equation for $u(r)$ in region I has the form

$$-\frac{\hbar^2}{2M} \left(\frac{d^2}{dr^2} - \frac{l(l+1)}{r^2} \right) u + \left(B - \frac{Ze_0^2}{\varepsilon_1 r} \right) u = Eu . \quad (35)$$

Eq. (35) resembles Eq. (19). In fact, with the replacements

$$Z \rightarrow \frac{Z}{\varepsilon_1} , \quad (36)$$

$$E \rightarrow E - B , \quad (37)$$

Eq. (19) becomes Eq. (35).

With the ansatz

$$u(r) = z_1^{l+1} w(z_1) e^{-\frac{z_1}{2}} \quad (38)$$

we obtain again Kummer's differential equation for $w(z)$

$$z_1 \frac{d^2 w}{dz_1^2} + (b_0 - z_1) \frac{dw}{dz_1} - a_1 w = 0 , \quad (39)$$

where b_0 is again given by (25) or (27), but a_1 is obtained from a_0 by the replacements (36), (37):

$$a_1 = \frac{2(l+1) - d_1}{2} , \quad (40)$$

$$d_1 = \frac{Ze_0^2}{\varepsilon_1 \hbar} \sqrt{\frac{2M}{|E - B|}} \quad (41)$$

and the dimensionless variable z_1 is related to r by

$$z_1 = 2 \cdot \sqrt{\frac{2M \cdot |E - B|}{\hbar^2}} r = 2\kappa_1 r . \quad (42)$$

The parameter κ_1 defined in (16) agrees with $\sqrt{2M/\hbar^2 \cdot |E - B|}$ because $E < 0$ and $B > 0$. The general solution w of Eq. (39) can be written as a linear combination of the function $U(a_1, 2l+2, z_1)$ and, as linearly independent 2nd solution, the confluent hypergeometric function $M(a_1, 2l+2, z_1)$:

$$w(z_1) = \tilde{A}_1 M(a_1, 2l+2, z_1) + \tilde{B}_1 U(a_1, 2l+2, z_1) . \quad (43)$$

We note that we had to suppress the solution $M(a_0, 2l+2, z_0)$ in region 0 because it would lead to a non-normalizable solution.

The radial solution $R(r)$ in region I thus assumes the form

$$R_I(r) = \frac{u(r)}{2\kappa_1 r} , \quad (44)$$

$$R_I(r) = (2\kappa_1 r)^l e^{-\kappa_1 r} \cdot [\tilde{A}_1 M(a_1, 2l+2, 2\kappa_1 r) + \tilde{B}_1 U(a_1, 2l+2, 2\kappa_1 r)] . \quad (45)$$

We now turn to the continuity conditions which enable us to determine the amplitudes A_I , B_I (or \tilde{A}_I , \tilde{B}_I), C_0 , and the energy eigenvalues E . Once these parameters will be obtained, we shall normalize the entire radial function to 1.

The radial wave function $R(r)$ and its 1st derivatives must be continuous at the limits $r = R_2$ and $r = R_1$ of the regions II and I:

$$R_{\text{II}}(R_2) = R_{\text{I}}(R_2) , \quad (46)$$

$$\frac{dR_{\text{II}}(R_2)}{dR_2} = \frac{dR_{\text{I}}(R_2)}{dR_2} , \quad (47)$$

$$R_{\text{I}}(R_1) = R_0(R_1) , \quad (48)$$

$$\frac{dR_{\text{I}}(R_1)}{dR_1} = \frac{dR_0(R_1)}{dR_1} . \quad (49)$$

We proceed as follows:

Eqs. (46) and (47) are 2 linear inhomogeneous equations for the amplitudes A_{I} , B_{I} (or \tilde{A}_{I} , \tilde{B}_{I}). We solve them for these amplitudes and substitute the result into the equation

$$\frac{d \ln R_{\text{I}}(R_1)}{dR_1} = \frac{d \ln R_0(R_1)}{dR_1} , \quad (50)$$

i.e. the ratio of the Eqs. (49) and (48). Eq. (50) represents a transcendental equation for the energy. It is solved numerically. The amplitude C_0 can subsequently be obtained from (48). The resulting wavefunction $R(r)$ is not yet normalized to 1. This can be easily achieved by the replacement

$$R(r) \rightarrow \tilde{R}(r) := \mathcal{N} \cdot R(r) , \quad (51)$$

with

$$\mathcal{N} = \left\{ \int_0^\infty dr r^2 R^2(r) \right\}^{-\frac{1}{2}} . \quad (52)$$

Let us present this procedure in more detail:

We introduce the abbreviations:

$$f_l^{(1)}(\kappa_{\text{I}}r) \equiv [f_l^{(1)}(x)]_{x=\kappa_{\text{I}}r} = \left[\sqrt{\frac{\pi}{2x}} I_{l+\frac{1}{2}}(x) \right]_{x=\kappa_{\text{I}}r} , \quad (53)$$

$$f_l^{(2)}(\kappa_{\text{I}}r) \equiv [f_l^{(2)}(x)]_{x=\kappa_{\text{I}}r} := \left[\sqrt{\frac{\pi}{2x}} K_{l+\frac{1}{2}}(x) \right]_{x=\kappa_{\text{I}}r} , \quad (54)$$

$$\tilde{f}_l^{(1)}(2\kappa_{\text{I}}r) \equiv [\tilde{f}_l^{(1)}(y)]_{y=2\kappa_{\text{I}}r} := \left[y^l e^{-\frac{y}{2}} M(a_{\text{I}}, 2l+2, y) \right]_{y=2\kappa_{\text{I}}r} , \quad (55)$$

$$\tilde{f}_l^{(2)}(2\kappa_{\text{I}}r) \equiv [\tilde{f}_l^{(2)}(y)]_{y=2\kappa_{\text{I}}r} := \left[y^l e^{-\frac{y}{2}} U(a_{\text{I}}, 2l+2, y) \right]_{y=2\kappa_{\text{I}}r} . \quad (56)$$

Furthermore, we use the prime ' to denote the derivative with respect to the variable given as argument:

$$f_l^{(i)'}(\kappa_{\text{I}}R_2) := \left[\frac{df_l^{(i)}(x)}{dx} \right]_{x=\kappa_{\text{I}}R_2} ,$$

$$\tilde{f}_l^{(i)'}(2\kappa_{\text{I}}R_2) := \left[\frac{d\tilde{f}_l^{(i)}(y)}{dy} \right]_{y=2\kappa_{\text{I}}R_2} ,$$

$$j_l'(\kappa_{\text{II}}R_2) := \left[\frac{dj_l(x)}{dx} \right]_{x=\kappa_{\text{II}}R_2} ,$$

a.s.o.

From the continuity equations (46), (47) we find the amplitudes A_I , B_I and \tilde{A}_I , \tilde{B}_I to be given by very similar relations

$$A_I = \frac{j_l(\kappa_{II}R_2)f_l^{(2)'}(\kappa_I R_2) - \frac{\kappa_{II}}{\kappa_I}f_l^{(2)}(\kappa_I R_2)j_l'(\kappa_{II}R_2)}{[W(f_l^{(1)}, f_l^{(2)})]_{\kappa_I R_2}}, \quad (57)$$

$$B_I = -\frac{j_l(\kappa_{II}R_2)f_l^{(1)'}(\kappa_I R_2) - \frac{\kappa_{II}}{\kappa_I}f_l^{(1)}(\kappa_I R_2)j_l'(\kappa_{II}R_2)}{[W(f_l^{(1)}(x), f_l^{(2)}(x))]_{x=\kappa_I R_2}}. \quad (58)$$

The Wronskian in the denominators is given by (see Ref. [5], Eq. (10.2.8))

$$W(f_l^{(1)}(x), f_l^{(2)}(x)) := f_l^{(1)}(x)f_l^{(2)'}(x) - f_l^{(2)}(x)f_l^{(1)'}(x) = -\frac{\pi}{2x^2}, \quad (59)$$

$$\tilde{A}_I = \frac{j_l(\kappa_{II}R_2)\tilde{f}_l^{(2)'}(2\kappa_I R_2) - \frac{\kappa_{II}}{2\kappa_I}\tilde{f}_l^{(2)}(2\kappa_I R_2)j_l'(\kappa_{II}R_2)}{[W(\tilde{f}_l^{(1)}(y), \tilde{f}_l^{(2)}(y))]_{y=2\kappa_I R_2}}, \quad (60)$$

$$\tilde{B}_I = -\frac{j_l(\kappa_{II}R_2)\tilde{f}_l^{(1)'}(2\kappa_I R_2) - \frac{\kappa_{II}}{2\kappa_I}\tilde{f}_l^{(1)}(2\kappa_I R_2)j_l'(\kappa_{II}R_2)}{[W(\tilde{f}_l^{(1)}(y), \tilde{f}_l^{(2)}(y))]_{y=2\kappa_I R_2}}. \quad (61)$$

The Wronskian in the denominators of (60) and (61) can be related to the Wronskian $W(M(a_I, 2l+2, y), U(a_I, 2l+2, y))$:

$$\begin{aligned} W(\tilde{f}_l^{(1)}(y), \tilde{f}_l^{(2)}(y)) &:= \tilde{f}_l^{(1)}(y)\tilde{f}_l^{(2)'}(y) - \tilde{f}_l^{(2)}(y)\tilde{f}_l^{(1)'}(y) \\ W(\tilde{f}_l^{(1)}(y), \tilde{f}_l^{(2)}(y)) &= y^{2l}e^{-y} \cdot W(M(a_I, 2l+2, y), U(a_I, 2l+2, y)) \end{aligned} \quad (62)$$

Using the differential Eq. (39), one finds for $W(M, U)$ (see Ref. [5], Eq. (13.1.22))

$$W(M(a_I, 2l+2, y), U(a_I, 2l+2, y)) = -\frac{\Gamma(2l+2) \cdot e^y}{\Gamma(a_I) \cdot y^{2l+2}} \quad (63)$$

and thus for $W(\tilde{f}_l^{(1)}(y), \tilde{f}_l^{(2)}(y))$:

$$W(\tilde{f}_l^{(1)}(y), \tilde{f}_l^{(2)}(y)) = -\frac{\Gamma(2l+2)}{\Gamma(a_I) \cdot y^2}. \quad (64)$$

Substituting (59) into (57) and (58) and, analogously, substituting (64) into (60) and (61) we obtain the following forms of the amplitudes in region I:

$$A_I = -\frac{2\kappa_I^2 R_2^2}{\pi} \left[j_l(\kappa_{II}R_2)f_l^{(2)'}(\kappa_I R_2) - \frac{\kappa_{II}}{\kappa_I}f_l^{(2)}(\kappa_I R_2)j_l'(\kappa_{II}R_2) \right], \quad (65)$$

$$B_I = \frac{2\kappa_I^2 R_2^2}{\pi} \left[j_l(\kappa_{II}R_2)f_l^{(1)'}(\kappa_I R_2) - \frac{\kappa_{II}}{\kappa_I}f_l^{(1)}(\kappa_I R_2)j_l'(\kappa_{II}R_2) \right], \quad (66)$$

$$\tilde{A}_I = -\frac{4\kappa_I^2 R_2^2 \Gamma(a_I)}{\Gamma(2l+2)} \left[j_l(\kappa_{II}R_2)\tilde{f}_l^{(2)'}(2\kappa_I R_2) - \frac{\kappa_{II}}{2\kappa_I}\tilde{f}_l^{(2)}(2\kappa_I R_2)j_l'(\kappa_{II}R_2) \right], \quad (67)$$

$$\tilde{B}_I = \frac{4\kappa_I^2 R_2^2 \Gamma(a_I)}{\Gamma(2l+2)} \left[j_l(\kappa_{II}R_2)\tilde{f}_l^{(1)'}(2\kappa_I R_2) - \frac{\kappa_{II}}{2\kappa_I}\tilde{f}_l^{(1)}(2\kappa_I R_2)j_l'(\kappa_{II}R_2) \right]. \quad (68)$$

With (65), (66) or (67), (68) the amplitudes of the 2 linearly independent solutions in region I are represented as a function of the energy E . The eigenvalues can now be obtained from the ratio of the two continuity conditions (49) and (48), i.e. from the equation

$$\left(\frac{d \ln R_I(r)}{dr}\right)_{r=R_1} = \left(\frac{d \ln R_0(r)}{dr}\right)_{r=R_1} . \quad (69)$$

This is a transcendental equation for the eigenenergies. It has infinitely many solutions close to the energy $E = 0$ due to the "infinite range" of the Coulomb potential. In spite of the complicated nature of the wavefunctions it is not difficult to find the numerical solutions of (69). More explicitly, the logarithmic derivatives in (69) look as follows:

$$\left[\frac{d \ln R_0(r)}{dr}\right]_{r=R_1} = \left[\frac{\frac{d}{dr}((2\lambda r)^l U(a_0, 2l + 2, 2\lambda r)e^{-\lambda r})}{(2\lambda r)^l U(a_0, 2l + 2, 2\lambda r)e^{-\lambda r}}\right]_{r=R_1} \quad (70)$$

$$\left[\frac{d \ln R_I(r)}{dr}\right]_{r=R_1} = \left[\frac{\frac{d}{dr}(A_I f_l^{(1)}(r) + B_I f_l^{(2)}(r))}{A_I f_l^{(1)}(r) + B_I f_l^{(2)}(r)}\right]_{r=R_1} \quad (71)$$

$$\left[\frac{d \ln R_I(r)}{dr}\right]_{r=R_1} = \left[\frac{\frac{d}{dr}(\tilde{A}_I \tilde{f}_l^{(1)}(r) + \tilde{B}_I \tilde{f}_l^{(2)}(r))}{\tilde{A}_I \tilde{f}_l^{(1)}(r) + \tilde{B}_I \tilde{f}_l^{(2)}(r)}\right]_{r=R_1} \quad (72)$$

Eq. (72) and (71) deal with the case of the exact potential and of the approximate constant potential in region I. In calculating the derivative $f_l^{(i)'}(r)$ or $\tilde{f}_l^{(i)'}(r)$ one can use properties of the different functions involved.

Having determined the eigenvalues from Eq. (69) one obtains the amplitude C_0 from Eq. (48) and thereafter the correct normalization of the entire function must be achieved by numerical calculation of the normalization constant (52).

3 Polarization effects in a macroscopic description

In Sec. 2, only the polarization of the insulator which is produced by a constant positive surface charge density $Z e_0 / (4\pi R_2^2)$ on the surface S_2 of the metal was taken into account. However, the charge distribution $\rho_e(\vec{r})$ of the externally localized electrons produces not only additional polarization effects in the insulating surface layer but also modifies the distribution of the positive surplus charge on the surface S_2 of the metal. In this section, we present a simple macroscopic description of the polarization effects which is based on Maxwell's equations in the presence of homogeneous dielectric media.

Outside of the metallic core, i.e. in the region I ($R_2 < r < R_1$) of the insulator, and in the vacuum 0 ($r > R_1$) surrounding the insulator the "electric field" \vec{E} and the "displacement" \vec{D} are related by:

$$\vec{D}(\vec{r}) = \varepsilon_I \vec{E}(\vec{r}) = (1 + 4\pi\chi_I) \vec{E}(\vec{r}) \quad \text{for } R_2 < r < R_1 \quad \text{region I} , \quad (73)$$

$$\vec{D}(\vec{r}) = \vec{E}(\vec{r}) \quad \text{for } r > R_1 \quad \text{region 0} , \quad (74)$$

where ε_I and χ_I are the "dielectric constant" and the "electric susceptibility" of the insulator, respectively. The fields satisfy Maxwell's equations

$$\text{div } \vec{D} = 4\pi\rho_e(\vec{r}) , \quad (75)$$

$$\text{rot } \vec{E} = 0 . \quad (76)$$

For the sake of simplicity, we assume that the distribution $\rho_e(\vec{r})$ of the externally located electrons and, as a consequence, also the positive surface charge distribution $\rho_{S_2}(\vec{r})$ on S_2 , are azimuthally symmetric, i.e. that they depend only on the polar angle ϑ and the radial coordinate r . They can thus be written in the form

$$\rho_e(\vec{r}) = \rho_e(r, \vartheta) = \sum_{l=0}^{\infty} \rho_l(r) Y_{l0}(\vartheta) , \quad (77)$$

$$\rho_{S_2}(\vec{r}) = \rho_{S_2}(R_2, \vartheta) = \sum_{l=0}^{\infty} \rho_l^{S_2} Y_{l0}(\vartheta) . \quad (78)$$

Integrating the surface charge density over the surface S_2 must yield the total positive surface charge Ze_0 . This implies the condition

$$Ze_0 = \int d^3r \delta(r - R_2) \rho_{S_2}(R_2, \vartheta) \quad (79)$$

or, with (78)

$$\rho_{l=0}^{S_2} = \frac{Ze_0}{\sqrt{4\pi}R_2^2} . \quad (80)$$

The components $\rho_l(r)$ of the electronic charge distribution are related to the total electronic charge distribution by

$$\rho_l(r) = 2\pi \int_0^\pi d\vartheta \sin \vartheta \rho_e(r, \vartheta) Y_{l0}(\vartheta) . \quad (81)$$

The Maxwell equations (75) and (76) are equivalent to the Poisson equation

$$\Delta \Phi_{\text{I}}(r, \vartheta) = -\frac{4\pi}{\varepsilon_{\text{I}}} \rho_e(r, \vartheta) \quad (82)$$

in region I and to

$$\Delta \Phi_{\text{0}}(r, \vartheta) = -4\pi \rho_e(r, \vartheta) \quad (83)$$

in region 0. Here, the potential

$$\Phi(r, \vartheta) = \Phi_{\text{I}}(r, \vartheta) \quad \text{for } R_2 < r < R_1 , \quad (84)$$

$$\Phi(r, \vartheta) = \Phi_{\text{0}}(r, \vartheta) \quad \text{for } r > R_1 \quad (85)$$

is related to the electric field \vec{E} by

$$\vec{E} = -\vec{\nabla} \Phi . \quad (86)$$

The following boundary conditions must be fulfilled at the surfaces S_2 and S_1 :

$$-\varepsilon_{\text{I}} \frac{\partial \Phi_{\text{I}}(R_2, \vartheta)}{\partial R_2} = 4\pi \rho_{S_2}(R_2, \vartheta) \quad (87)$$

$$\frac{\partial \Phi_{\text{I}}(R_2, \vartheta)}{\partial \vartheta} = 0 \quad (88)$$

$$\varepsilon_{\text{I}} \frac{\partial \Phi_{\text{I}}(R_1, \vartheta)}{\partial R_1} = \frac{\partial \Phi_{\text{0}}(R_1, \vartheta)}{\partial R_1} \quad (89)$$

$$\Phi_I(R_1, \vartheta) = \Phi_0(R_1, \vartheta). \quad (90)$$

Furthermore, the potential $\Phi_0(r, \vartheta)$ must satisfy the asymptotic condition

$$\Phi_0(r, \vartheta) \rightarrow 0 \left(\frac{1}{r} \right). \quad (91)$$

The conditions (87) and (89) are obtained from the Maxwell equation (75), and the conditions (88) and (90) result from (76) and the requirement that the classical electric field should be everywhere finite.

The solutions Φ_I and Φ_0 of the Poisson equations (82) and (83) in the regions I and 0, respectively, can be written in the form:

$$\Phi_I(r, \vartheta) = \frac{1}{\varepsilon_I} \Psi(r, \vartheta) + \varphi_I(r, \vartheta), \quad (92)$$

$$\Phi_0(r, \vartheta) = \Psi(r, \vartheta) + \varphi_0(r, \vartheta), \quad (93)$$

where $\Psi(r, \vartheta)$ is the Coulomb potential produced by the electronic charge distribution $\rho_e(\vec{r}', \vartheta')$

$$\Psi(r, \vartheta) := \int d^3r' \frac{\rho_e(r', \vartheta')}{|\vec{r} - \vec{r}'|}. \quad (94)$$

The charge distribution $\rho_e(\vec{r})$ itself is to be calculated from the wavefunctions of the bound and predominantly externally located (i.e. in region 0, $r > R_1$) electrons. The "conduction electrons" which are located internally (i.e. in region II, $r < R_2$) do not contribute to $\rho_e(\vec{r})$ because they are already taken into account by the number Z of positive surplus charges. The density $\rho_e(\vec{r})$ is thus mainly located in region 0 and it is very small in region I, i.e. inside of the insulating surface layer, because the eigenenergies of the electrons are far below the positive barrier in region I.

The function $\varphi_I(r, \vartheta)$ is the general azimuthally symmetric solution of the Laplace equation in region I

$$\varphi_I(r, \vartheta) = \sum_{l=0}^{\infty} \left(C_l^I r^l + \frac{D_l^I}{r^{l+1}} \right) Y_{l0}(\vartheta) \quad (95)$$

and $\varphi_0(r, \vartheta)$ the corresponding most general solution of the Laplace equation in region 0 satisfying in addition the asymptotic condition (91):

$$\varphi_0(r, \vartheta) = \sum_{l=0}^{\infty} \frac{D_l^0}{r^{l+1}} Y_{l0}(\vartheta). \quad (96)$$

The Coulomb potential $\Psi(r, \vartheta)$ can be written as

$$\Psi(r, \vartheta) = \sum_{l=0}^{\infty} \frac{4\pi}{2l+1} \left(a_l(r) r^l + \frac{b_l(r)}{r^{l+1}} \right) Y_{l0}(\vartheta), \quad (97)$$

where the functions $a_l(r)$ and $b_l(r)$ are related to the components $\rho_l(r)$ of the electronic charge distribution by

$$a_l(r) := \int_r^{\infty} dr' \rho_l(r') r'^{1-l}, \quad (98)$$

$$b_l(r) := \int_0^r dr' \rho_l(r') r'^{l+2}. \quad (99)$$

Substituting the explicit forms (95) to (97) into the boundary conditions (87), (89), and (90), we obtain the relations

$$-\sum_{l=0}^{\infty} \left\{ \frac{4\pi}{(2l+1)\varepsilon_1} \left(a_l(R_2)lR_2^{l-1} - \frac{b_l(R_2)(l+1)}{R_2^{l+2}} \right) + C_l^I l R_2^{l-1} - \frac{D_l^I \cdot (l+1)}{R_2^{l+2}} + \frac{4\pi}{\varepsilon_1} \rho_l^{S_2} \right\} Y_{l0}(\vartheta) = 0, \quad (100)$$

$$\varepsilon_1 \sum_{l=0}^{\infty} \left\{ C_l^I l R_1^{l-1} - \frac{D_l^I \cdot (l+1)}{R_1^{l+2}} + \frac{D_l^0 \cdot (l+1)}{R_1^{l+2}\varepsilon_1} \right\} Y_{l0}(\vartheta) = 0, \quad (101)$$

$$\sum_{l=0}^{\infty} \left\{ C_l^I R_1^l + \frac{D_l^I}{R_1^{l+1}} - \frac{D_l^0}{R_1^{l+1}} \right\} Y_{l0}(\vartheta) = 0. \quad (102)$$

Furthermore, using the identity (see for instance Ref. [5]) for $l \geq 1$

$$\sin \vartheta \frac{dY_{l0}}{d\vartheta} = \frac{l(l+1)}{\sqrt{2l+1}} \left[\frac{Y_{l+1,0}}{\sqrt{2l+3}} - \frac{Y_{l-1,0}}{\sqrt{2l-1}} \right] \quad (103)$$

together with (92), (93) and (95), the condition (88) can be shown to be equivalent to the relation

$$\frac{4\pi}{(2l+1)\varepsilon_1} \left(a_l(R_2)R_2^l + \frac{b_l(R_2)}{R_2^{l+1}} \right) + C_l^I R_2^l + \frac{D_l^I}{R_2^{l+1}} = 0, \quad (104)$$

where $l \geq 1$. Eq. (104) is seen to imply that the potential $\Phi_1(r, \vartheta)$ is constant on the surface S_2 . For $l = 0$, we obtain from (100)

$$D_0^I = \frac{4\pi}{\varepsilon_1} [-b_0(R_2) + R_2^2 \rho_0^{S_2}] \quad (105)$$

and from (101) and (102) the relations

$$\varepsilon_1 D_0^I = D_0^0, \quad (106)$$

$$C_0^I + \frac{D_0^I}{R_1} = \frac{D_0^0}{R_1}. \quad (107)$$

Hence, with (105), we find

$$C_0^I = \frac{(\varepsilon_1 - 1)4\pi}{\varepsilon_1 R_1} [-b_0(R_2) + R_2^2 \rho_0^{S_2}] \quad (108)$$

and

$$D_0^0 = 4\pi [-b_0(R_2) + R_2^2 \rho_0^{S_2}]. \quad (109)$$

For $l \geq 1$, we obtain from (100) and (104):

$$C_l^I = -\frac{4\pi}{(2l+1)\varepsilon_1} \left[a_l(R_2) + \frac{\rho_l^{S_2}}{R_2^{l-1}} \right], \quad (110)$$

$$D_l^I = \frac{4\pi}{(2l+1)\varepsilon_1} [-b_l(R_2) + \rho_l^{S_2} R_2^{l+1}]. \quad (111)$$

For the coefficients D_l^0 , we find the relations

$$D_l^0 = C_l^I R_1^{2l+1} + D_l^I \quad (112)$$

and

$$D_l^0 = \varepsilon_I \left[-C_l^I \cdot \frac{l}{(l+1)} R_1^{2l+1} + D_l^I \right] \quad (113)$$

from the Eqs. (102) and (101), which hold for $l \geq 0$.

The equality of the righthand sides of (112) and (113) together with (110) and (111) yields a condition for the surface charge components $\rho_l^{S_2}$ for $l \geq 1$. From this equation one finds the explicit form

$$\rho_l^{S_2} = R_2^{l-1} \frac{\left\{ -a_l(R_2) \left(\frac{l}{l+1} \varepsilon_I + 1 \right) + b_l(R_2) R_1^{-(2l+1)} \cdot (\varepsilon_I - 1) \right\}}{\left\{ \left(\frac{l}{l+1} \varepsilon_I + 1 \right) + \left(\frac{R_2}{R_1} \right)^{2l+1} (\varepsilon_I - 1) \right\}} \quad (114)$$

for $l \geq 1$. The component $\rho_0^{S_2}$ is determined by the conservation of the total positive charge on S_2 and is given by Eq. (80).

For $l \geq 1$, one obtains from (110), (111) and (113)

$$D_l^0 = \frac{4\pi}{(2l+1)} \left\{ \frac{l}{l+1} R_1^{2l+1} a_l(R_2) - b_l(R_2) + \rho_l^{S_2} \cdot \left(\frac{l}{l+1} \frac{R_1^{2l+1}}{R_2^{l-1}} + R_2^{l+2} \right) \right\} \quad (115)$$

As we have mentioned already, the charge distribution $\rho_e(r, \vartheta)$ of the externally located electrons is vanishingly small for $r < R_1$. Consequently, we have

$$b_l(r) \approx 0 \quad \text{for} \quad r < R_1 \quad (116)$$

and

$$a_l(r) \approx a_l(R_1) \quad \text{for} \quad r < R_1. \quad (117)$$

The potentials $\Phi_0(\vec{r})$, $\Phi_I(\vec{r})$, $\Phi_{II} = \Phi_I(R_2)$, and the charge distribution $\rho_{S_2}(R_2, \vartheta)$ on the surface S_2 are thus fully determined for a given azimuthally symmetric distribution $\rho_e(r, \vartheta)$ of the externally located electrons.

The potential $\tilde{V}(\vec{r})$ acting on an electron in our "mesoscopic atom" is related to the potential functions as follows:

$$\tilde{V}(r, \vartheta) = -e_0 \Phi_{II} - V_{II}^0 = -e_0 \Phi_I(R_2) - V_{II}^0 \quad \text{for} \quad r < R_2, \quad (118)$$

$$\tilde{V}(r, \vartheta) = -e_0 \Phi_I(r, \vartheta) + B_0 \quad \text{for} \quad R_2 < r < R_1, \quad (119)$$

$$\tilde{V}(r, \vartheta) = -e_0 \Phi_0(r, \vartheta) \quad \text{for} \quad r > R_1 \text{ (region 0)}. \quad (120)$$

The potential $(-V_{II}^0)$ represents the interaction of a conduction electron with the average ionic background charge in the metal and has to be added to the constant potential $-e_0 \Phi_{II}$ produced by the positive surplus charge on S_2 . The potential barrier B_0 to be added in the insulating surface layer is related to the average energy gap between the electronic bands. Since it is of quantum mechanical origin, it is not contained in the classically determined term $-e_0 \Phi_I(r, \vartheta)$.

The Schrödinger equation with the potential $\tilde{V}(r, \vartheta)$ can no longer be solved analytically. One could diagonalize the Hamiltonian

$$\hat{H} = -\frac{\hbar^2}{2M} \Delta + \tilde{V}(r, \vartheta) \quad (121)$$

within the set of analytical eigenfunctions which we have determined in Sec. 2. This represents a selfconsistency problem, because the eigenfunctions of the Hamiltonian (121) depend on the charge distribution $\rho_e(\vec{r})$ which is calculated from them. The solution thus requires an iteration process.

Let us consider two special cases for which the results of this section simplify considerably:

1. If we neglect the polarization effects produced by the external electrons, that is if we put

$$\rho_e(\vec{r}) = 0, \quad (122)$$

the quantities $a_l(r)$, $b_l(r)$ vanish for $l \geq 0$, and, as a consequence, so do the components $\rho_{l \geq 1}^{S_2}$. The positive surplus charge density on S_2 is then spherically symmetric and given by

$$\rho_{S_2}(r, \vartheta) = \rho_0^{S_2} Y_{00} = \frac{Ze_0}{4\pi R_2^2}. \quad (123)$$

It is easily seen that, in this case, the potential $V(r, \vartheta)$ becomes equal to the potential $V(r)$ we considered in Sec. 2.

2. If we assume that the charge density $\rho_e(\vec{r})$ of the external electrons is spherically symmetric

$$\rho_e(\vec{r}) = \rho_e(r), \quad (124)$$

only the component $\rho_{l=0}(r)$ in (77) is unequal 0

$$\rho_l(r) = \delta_{l0} \cdot \sqrt{4\pi} \rho_e(r) \quad (125)$$

and, consequently, the quantities $a_l(r)$, $b_l(r)$, and $\rho_l^{S_2}$ vanish for $l \geq 1$. In this case, the potentials Φ_{II} , Φ_I and Φ_0 take the following form

$$\Phi_{II} = \Phi_I(R_2) \quad (\text{for } r < R_2), \quad (126)$$

$$\Phi_I(r) = \left(a_0(r) + \frac{b_0(r)}{r} \right) \sqrt{4\pi} + \frac{(\varepsilon_I - 1) Ze_0}{\varepsilon_I R_1} + \frac{Ze_0}{\varepsilon_I r} \quad (\text{for } R_2 < r < R_1), \quad (127)$$

$$\Phi_0(r) = \left(a_0(r) + \frac{b_0(r)}{r} \right) \sqrt{4\pi} + \frac{Ze_0}{r} \quad (\text{for } r > R_1). \quad (128)$$

The case of a spherically symmetric distribution of the externally located electrons is realistic at finite temperature, because magnetic substates of a given electronic level are expected to be occupied with the same probability whenever the mesoscopic atom is in contact with a thermal reservoir of finite temperature.

The functions $a_0(r)$ and $b_0(r)$ depend themselves on the electronic distribution. For $r \gg R_1$, $a_0(r)$ decreases to zero as one can see from (98). The quantity $\sqrt{4\pi} b_0(r)$ represents the total charge of the externally located electrons inside the sphere of radius r

$$Q_e(r) := \int_0^r dr' r'^2 \int d\Omega' \rho_e(r', \vartheta'). \quad (129)$$

Using (77) in (129) we find

$$\sqrt{4\pi} b_0(r) = Q_e(r). \quad (130)$$

For $r \gg R_1$, $\sqrt{4\pi} b_0(r)$ tends to the total charge $Q_e(\infty)$ of the externally located electrons.

If the mesoscopic atom is neutral, i.e. if there are as many externally bound electrons as there are positive surplus charges on the surface S_2 of the metallic core, the term $b_0(r)\sqrt{4\pi}/r$ in Eq. (128) cancels the potential Ze_0/r for $r \gg R_1$, as it should.

Let us study the asymptotic behaviour of the function $a_0(r)$ and $b_0(r)$ for $r \rightarrow \infty$: For simplicity, let us assume that only the lowest external electron state is occupied by two electrons,

one with intrinsic spin up and the other one with spin down. The external state of lowest energy belongs necessarily to orbital angular momentum ($l = 0$) and to zero number of radial modes. We assume that the wavefunctions we determined in Sec. 2 are realistic for $r \gg R_1$. In region 0, the electronic density distribution is then given by

$$\rho_e(r) = (-e_0) \cdot 2R_{l=0}^2(r; E) Y_{00}^2 = \frac{(-e_0)}{2\pi} \left(\frac{u_{l=0}(2\lambda r)}{2\lambda r} \right)^2 \quad (131)$$

or, substituting the explicit wavefunction (20), by

$$\rho_e(r) = \frac{(-e_0)}{2\pi} C_0^2 \mathcal{N}^2 U^2 \left(\frac{2-d_0}{2}, 2, 2\lambda r \right) e^{-2\lambda r}. \quad (132)$$

Here, \mathcal{N} is the overall normalization constant introduced by Eq. (52).

For $z_0 \gg 1$, the function $U(a_0, b_0, Z_0)$ can be replaced by (see Ref. [5], Eq. (13.5.2))

$$U(a_0, b_0, z_0)_{z_0 \gg 1} \approx \frac{1}{z_0^{a_0}} \left\{ 1 + \sum_{n=1}^{\infty} \frac{(a_0)_n (1+a_0-b_0)_n}{n!} \left(\frac{1}{-z_0} \right)^n \right\}. \quad (133)$$

Retaining only the 1st term in (133), we obtain for the asymptotic density ($2\lambda r \ll 1$)

$$\rho_e(r) \approx \frac{(-e_0)(C_0 \mathcal{N})^2}{2\pi} (2\lambda r)^{d_0-2} e^{-2\lambda r} \quad (134)$$

and for the function $a_0(r)$

$$a_0(r) \approx \sqrt{4\pi} \int_r^{\infty} dr' r' \rho_e(r') = \frac{(-e_0)(C_0 \mathcal{N})^2}{\sqrt{\pi}(2\lambda)^2} \int_{2\lambda r}^{\infty} dz_0 (z_0)^{d_0-1} e^{-z_0} \quad (135)$$

The integral in (135) is the "incomplete Γ -function" (see Ref. [5], Eq. (6.5.3), $Re(a) > 0$)

$$\Gamma(a, x) := \int_x^{\infty} dt t^{a-1} e^{-t} \quad (136)$$

with the asymptotic expansion (Ref. [5], Eq. (6.5.32))

$$\Gamma(a, x) \approx x^{a-1} e^{-x} \left\{ 1 + \frac{a-1}{x} + \frac{(a-1)(a-2)}{x^2} + \dots \right\}. \quad (137)$$

From (135)–(137), we obtain $a_0(r)$ in the form

$$a_0(r) \approx \frac{(-e_0)(C_0 \mathcal{N})^2}{\sqrt{\pi}(2\lambda)^2} (2\lambda r)^{d_0-1} e^{-2\lambda r} \quad (138)$$

for $2\lambda r \geq 1$.

Of course, one could raise the accuracy of the result (138) by incorporating one or two more terms in (133) and (137). The important point, however, is that $a_0(r)$ tends to zero exponentially for large values of $r \gg R_1$. This justifies the assumption that the electronic charge density $\rho_e(r)$ in the asymptotic regime $r \gg R_1$ is correctly described by the wavefunctions of Sec. 2, which do not contain the electronic polarization effects.

The function $b_0(r)$ can be written in the form (see (99))

$$b_0(r) = \sqrt{4\pi} \int_0^\infty dr' r'^2 \rho_e(r') - \sqrt{4\pi} \int_r^\infty dr' r'^2 \rho_e(r') , \quad (139)$$

with

$$\int_0^\infty dr' r'^2 \rho_0(r') = \sqrt{4\pi} \int_0^\infty dr' r'^2 \rho_e(r') = \frac{Q_e(\infty)}{\sqrt{4\pi}} . \quad (140)$$

The 2nd term on the r.h.s. of (139) is easily seen to have the approximate form

$$\int_0^\infty dr' r'^2 \rho_0(r') \approx \frac{(-e_0)(C_0\mathcal{N})^2}{\sqrt{\pi}(2\lambda)^3} (2\lambda r)^{d_0} e^{-2\lambda r} \quad (141)$$

for $2\lambda r \geq 1$.

Thus the function $b_0(r)$ is asymptotically ($2\lambda r \geq 1$) given by

$$b_0(r) = \frac{Q_{el}(\infty)}{\sqrt{4\pi}} + \frac{e_0(C_0\mathcal{N})^2}{\sqrt{\pi}(2\lambda)^3} (2\lambda r)^{d_0} \cdot e^{-2\lambda r} , \quad (142)$$

which means that it approaches exponentially the asymptotic value $Q_e(\infty)/\sqrt{4\pi}$.

In the general case of a ϑ -dependent electronic charge density $\rho_e(r, \vartheta)$, the quantities $a_{l \neq 0}(r)$ and $b_{l \neq 0}(r)$ are different from zero and their asymptotic behaviour can be investigated in an analogous way. One finds that $a_{l > 0}(r)$ tends exponentially to zero and $b_{l > 0}(r)$ exponentially to constant values as r goes to infinity. Therefore, at large values of r , the dominant part of the potential $\tilde{V}(r, \vartheta)$ is the potential $V(r)$ given by Eq. (6). Thereby, our assumption that the wavefunctions determined in Sec. 2 are essentially correct at large values of λr is seen to be justified.

For non-asymptotic values of r , the electronic charge density and the resulting functions $a_0(r)$ and $b_0(r)$ must be obtained from the eigenfunctions of the Hamiltonian (120) which contains the potential $\tilde{V}(r, \vartheta)$ defined in (118) to (120). Let us formulate the special case of a spherically symmetric charge density and the resulting spherically symmetric potential $V(r)$ in somewhat more detail:

The electronic charge density at a finite temperature T is given by

$$\rho_e(\vec{r}) = -e_0 \sum_{n=1}^{\infty} \sum_{l=0}^{\infty} \left\{ \frac{2}{\exp\left(\frac{E_{nl}-\mu}{T}\right) + 1} \right\} R_l^2(r; E_{nl}) \sum_{m=-l}^l |Y_{lm}(\vartheta, \varphi)|^2 \quad (143)$$

or, using the relation (see for instance Ref. [7], Eq. (3.69))

$$\sum_{m=-l}^{+l} |Y_{lm}(\vartheta, \varphi)|^2 = \frac{(2l+1)}{4\pi} \quad (144)$$

by

$$\rho_e(r) = -e_0 \sum_{n=1}^{\infty} \sum_{l=0}^{\infty} \frac{(2l+1)}{2\pi} \cdot \frac{1}{\left\{ \exp\left(\frac{E_{nl}-\mu}{T}\right) + 1 \right\}} \cdot R_l^2(r; E_{nl}) . \quad (145)$$

Here, E_{nl} is the n -th eigenvalue for given angular momentum l and $R_l(r; E_{nl})$ is the corresponding eigenfunction of the radial Schrödinger equation. The parameter μ represents the chemical

potential which corresponds to the number of externally located electrons.

The potential $\tilde{V}(r, \vartheta)$ has the form

$$\tilde{V}(r) = -e_0\Phi_1(R_2) - V_{\text{II}}^0 \quad \text{for } r_2 < R_2, \quad (146)$$

$$\begin{aligned} \tilde{V}(r) &= -e_0\Phi_1(r) + B_0 \\ &= B_0 - e_0 \left\{ \frac{4\pi}{\varepsilon_1} \left(a_0(r) + \frac{b_0(r)}{r} \right) + C_0^I + \frac{D_0^I}{r} \right\} Y_{00} \quad \text{for } R_2 < r < R_1, \end{aligned} \quad (147)$$

$$\tilde{V}(r) = -e_0\Phi_0(r) = -e_0 \left\{ 4\pi \left(a_0(r) + \frac{b_0(r)}{r} \right) + \frac{D_0^0}{r} \right\} Y_{00} \quad \text{for } r > R_1, \quad (148)$$

where D_0^I , C_0^I , and D_0^0 are given by the Eq. (105), (108), and (109), resp. The functions $a_0(r)$ and $b_0(r)$ are defined by (98) and (99), where $\rho_0(r') = \sqrt{4\pi}\rho_e(r')$. The wavefunctions $R_l(r; E_{nl})$ are solutions of the radial Schrödinger equation with $\tilde{V}(r)$ given by (146) - (148)

$$\left\{ -\frac{\hbar^2}{2M} \left(\frac{d^2}{dr^2} + \frac{2}{r} \frac{d}{dr} - \frac{l(l+1)}{r^2} \right) + \tilde{V}(r) - E_{nl} \right\} \tilde{R}_l(r; E_{nl})_l. \quad (149)$$

Since $\tilde{V}(r)$ depends itself on the functions $\tilde{R}_l(r; E_{nl})$, one has to solve (149) by iteration. One way to find the solutions $\tilde{R}_l(r; E_{nl})$ of (149) is to expand the solutions $R_l(r; E_{nl})$ in terms of the radial eigenfunctions $R_l(r; \overset{\circ}{E}_0)$ defined in Sec. 2, where the potential $V(r)$ is given by Eq. (5) and related to $\tilde{V}(r)$ by

$$V(r) = \lim_{\rho_e(r) \rightarrow 0} \tilde{V}(r) \quad (150)$$

$$\tilde{R}_l(r; E_{nl}) = \sum_{\nu} c_{\nu} R_l(r; \overset{\circ}{E}_{\nu}) \quad (151)$$

$\overset{\circ}{E}_{\nu}$ are the eigenvalues obtained in Sec. 2. In Eq. (151) we left away the basis functions $R_l(r, E)$ corresponding to continuous eigenvalues $\overset{\circ}{E}$ of Eq. (9). Substitution of (151) into (149) leads to a nonlinear system of equations for the expansion coefficients c_{ν} which must be solved by iteration.

4 Results

We present results on the spectrum of eigenenergies, the eigenfunctions, and on the electromagnetic transition rate between externally and internally localized states for a range of values of the parameters R_1 , R_2 , and ε_I . So far, we have not taken into account the effects presented in Sec. 3, i.e. the polarization of the insulating dielectric material by externally localized electrons. The additional potential produced by this polarization is expected to modify the wave functions in the vicinity of the surface S_1 , perhaps even rather substantially. At large distances (say a couple of Ångström outside of the surface S_1), the additional polarization potential tends rapidly to zero. Consequently, the wavefunctions presented in this article are expected to be trustworthy at distances of a couple of Ångström from the surface S_1 .

4.1 Eigenfunctions and eigenenergies

We studied only the case that the Coulomb potential $-Ze_0^2/(r\varepsilon_I)$ within the insulator ($R_2 \leq r \leq R_1$) is small compared to the barrier height B which is related to the gap parameter B_0 by Eq. (4). This means that we neglected the Coulomb potential in region I.

Table 1: The energies $Ze_0^2/(R_2\varepsilon_1)$, $Ze_0^2(\varepsilon_1 - 1)/(R_1\varepsilon_1)$, and the barrier height B as a function of the radii R_1 and R_2 and of the dielectric constant ε_1 . Energies are given in meV and radii in Å. The parameter B_0 is chosen equal to 2500 meV or 4000 meV.

R_2 (Å)	20	20	20	10	10	10	3.5	3.5
R_1 (Å)	28	28	28	18	18	18	10	10
ε_1	115 (TiO ₂)	28 (Hg0)	10 (Al ₂ O ₃)	115 (TiO ₂)	28 (Hg0)	10 (Al ₂ O ₃)	115 (TiO ₂)	10 (Al ₂ O ₃)
Z	1	1	1	1	1	1	1	1
$\frac{Ze_0^2}{R_2\varepsilon_1}$ (meV)	6.26	25.7	72	12.5	51.4	144	35.8	411
$\frac{Ze_0^2(\varepsilon_1-1)}{R_1\varepsilon_1}$ (meV)	509.8	495.9	462.9	793	771	720	1427	1296
B (meV) for $B_0 = 4000$	3490	3504	3537	3207	3229	3280	2573	2704
B (meV) for $B_0 = 2500$	1990	2004	2037	1707	1729	1780	1073	1204

In Table 1 we present the energies $Ze_0^2/(R_2\varepsilon_1)$, $Ze_0^2(\varepsilon_1 - 1)/(R_1\varepsilon_1)$, and the barrier height B for typical values of the parameters $R_{1,2}$ and ε_1 . It is seen that neglecting the screened Coulomb potential $Ze_0^2/(R_1\varepsilon_1)$ in region I as compared to B is sometimes a very good approximation, but, not in general, especially not for $Z > 1$ and for radii $R_{1,2} \leq 10$ Å.

The eigenvalues were determined by a numerical solution of the eigenvalue equation (69) using the form of $d \ln R_I(R_1)/dR_1$ as given by the Eq. (71), (65), and (66). Up to the common normalization factor \mathcal{N} (see (52)), the radial eigenfunctions $R(r; l, E)$ are then obtained from the equations (11), (18), and (20) in the regions II, I, and 0, resp.

In order to simplify the comparison of results which correspond to different choices of the parameters $R_{1,2}$, B , V_{II} and Z , it is advantageous to use the energy unit Ze_0^2/R_1 , i.e. the value of the Coulomb potential at the outer surface S_1 . The resulting dimensionless quantities are denoted by

$$\varepsilon := \frac{E}{Ze_0^2/R_1}, \quad (152)$$

$$b := \frac{B}{Ze_0^2/R_1}, \quad (153)$$

$$v_{II} := \frac{V_{II}}{Ze_0^2/R_1}, \quad (154)$$

$$\varepsilon_{\max} := \frac{(V_{II} + Ze_0^2/R_2)}{Ze_0^2/R_1} = \frac{E_{\max}}{Ze_0^2/R_1} = v_{II} + \frac{R_1}{R_2}. \quad (155)$$

Furthermore, it is convenient to introduce the typical length parameters R_0 and R_{00} ($= 0,264589$ Å):

$$R_0 := \frac{\hbar^2}{2Me_0^2Z} \equiv \frac{R_{00}}{Z}. \quad (156)$$

In what follows we give some technical details concerning the determination of the eigenvalues and eigenenergies.

In region I, due to our approximation, the radial eigenfunction R_I is given by Eq. (18), i.e. as a linear superposition of the modified spherical Bessel functions $f_l^{(1)}(x)$ and $f_l^{(2)}(x)$ defined

in (53) and (54) with $x \equiv \kappa_I r$. We calculate these functions by representing them in the form (see Ref. [5], Chapt. 10)

$$f_l^{(1)}(x) = \frac{1}{2x} \left[R\left(l + \frac{1}{2}, -x\right) e^x + (-1)^l R\left(l + \frac{1}{2}, x\right) e^{-x} \right], \quad (157)$$

$$f_l^{(2)}(x) = \frac{\pi}{2x} R\left(l + \frac{1}{2}, x\right) e^{-x} \quad (158)$$

as a linear superposition of exponentially rising and decreasing terms. Here, the function $R\left(l + \frac{1}{2}, x\right)$ is defined (see Ref. [5], Eq. (10.2.11)) as

$$R\left(l + \frac{1}{2}, x\right) := \sum_{k=0}^l \binom{l + \frac{1}{2}}{k} (2x)^{-k}, \quad (159)$$

$$\binom{l + \frac{1}{2}}{k} := \frac{(l + k)!}{k!(l - k)!}.$$

It turned out to be convenient to rewrite $R_I(r)$ in the form

$$R_I(r) = A'_I g_l^{(1)}(x) e^{x - \kappa_I R_2} + \frac{1}{\pi} \left[B'_I + (-1)^l A'_I e^{-2\kappa_{II} R_2} \right] \cdot g_l^{(2)}(x) e^{-(x - \kappa_I R_2)}, \quad (160)$$

where the functions $g_l^{(1,2)}(x)$ are related to $f_l^{(1,2)}(x)$ by

$$g_l^{(1)}(x) := f_l^{(1)}(x) e^{-x}, \quad (161)$$

$$g_l^{(2)}(x) := f_l^{(2)}(x) e^x. \quad (162)$$

The amplitudes A'_I, B'_I are connected with the amplitudes A_I and B_I of Eq. (18) by

$$A'_I = A_I e^{\kappa_I R_2}, \quad (163)$$

$$B'_I = [(-1)^{l+1} A_I + \pi B_I] e^{-\kappa_I R_2}. \quad (164)$$

The advantage of using (160) instead of (18) is that the functions $g_l^{(1,2)}(y)$ can be numerically determined more comfortably than the functions $f_l^{(1,2)}(y)$ and that they have a simpler asymptotic behaviour

$$g_l^{(1)}(x) \rightarrow \frac{1}{2x} + O\left(\frac{1}{x^2}\right), \quad (165)$$

$$g_l^{(2)}(x) \rightarrow \frac{\pi}{2x} + O\left(\frac{1}{x^2}\right). \quad (166)$$

From the continuity conditions (46), (47) one obtains A'_I and B'_I in the form

$$A'_I = -\frac{2}{\pi} (\kappa_I R_2)^2 \left[dg_l^{(2)}(\kappa_I R_2) \cdot j_l(\kappa_{II} R_2) - \frac{\kappa_{II}}{\kappa_I} g_l^{(2)}(\kappa_I R_2) j'_l(\kappa_{II} R_2) \right], \quad (167)$$

$$B'_I = (-1)^{l+1} A'_I e^{-2\kappa_I R_2} + 2(\kappa_I R_2)^2 \left[dg_l^{(1)}(\kappa_I R_2) j_l(\kappa_{II} R_2) - \frac{\kappa_{II}}{\kappa_I} g_l^{(1)}(\kappa_I R_2) j'_l(\kappa_{II} R_2) \right], \quad (168)$$

where the function $dg^{(1,2)}(x)$ are defined by

$$dg^{(1)}(x) = e^{-x} f_l^{(1)'}(x) , \quad (169)$$

$$dg^{(2)}(x) = e^{+x} f_l^{(2)'}(x) . \quad (170)$$

Then, the continuity condition (69) assumes the explicit form

$$\begin{aligned} F(\varepsilon) : &= U \left(l + 1 - \frac{d_0}{2}, 2l + 2, 2\lambda R_1 \right) [lR_1 + \kappa_I R_1 \tilde{R}_1] \\ &+ 2\lambda R_1 \cdot (l + 1 - \frac{d_0}{2}) U \left(l + 2 - \frac{d_0}{2}, 2l + 3, 2\lambda R_1 \right) \cdot R_1 \\ &+ (\lambda R_1 - l) U \left(l + 1 - \frac{d_0}{2}, 2l + 2, 2\lambda R_1 \right) \cdot R_1 = 0 \end{aligned} \quad (171)$$

with

$$R_I := R_1(R_1) , \quad (172)$$

$$\begin{aligned} \tilde{R}_I : &= A_I' g_{l+1}^{(1)}(\kappa_I R_1) e^{\kappa_I(R_1 - R_2)} - \frac{1}{\pi} B_I' g_{l+1}^{(2)}(\kappa_I R_1) e^{-\kappa_I(R_1 - R_2)} \\ &- \frac{(-1)^{l+1}}{\pi} A_I' g_{l+1}^{(2)}(\kappa_I R_1) e^{-\kappa_I(R_1 - R_2)} e^{-2\kappa_I R_2} . \end{aligned} \quad (173)$$

In terms of the dimensionless parameters (152) to (155) the arguments which appear in the transcendental equation (171) take the form

$$\kappa_I R_1 = \sqrt{\frac{R_1}{R_0}} \sqrt{b + |\varepsilon|} , \quad (174)$$

$$\kappa_{II} R_2 = \sqrt{\frac{R_2}{R_0}} \sqrt{\frac{R_2}{R_1}} \sqrt{b + |\varepsilon|} = \sqrt{\frac{R_2}{R_0}} \sqrt{\frac{R_2}{R_1}} \sqrt{\varepsilon_{\max} - |\varepsilon|} , \quad (175)$$

$$\lambda R_1 = \sqrt{\frac{R_1}{R_0}} \sqrt{\varepsilon} , \quad (176)$$

$$d_0 = \sqrt{\frac{R_1}{R_0}} \frac{1}{\sqrt{\varepsilon}} . \quad (177)$$

We determined the zeros of the function $F(\varepsilon)$ by calculating numerically $F(\varepsilon)$ in small steps of ε between limits ε_{\min} and ε_{\max} . Whenever $F(\varepsilon)$ changed sign from a given step to the next one, we refined the mesh by usually a factor of 100 so as to determine the zero with the desired accuracy. We note that, for each given value of the angular momentum l , there is an infinity of eigenvalues as ε approaches $\varepsilon = 0$ from below. This is so as a result of the infinite range of the Coulomb potential in region 0. In the domain of small $|\varepsilon|$, i.e. of very weakly bound electrons, and also for large well depth v_{II} , the function $F(\varepsilon)$ oscillates between large positive and negative values. Nevertheless, for a sufficiently narrow system of mesh points, the function $F(\varepsilon)$ is of reasonable size for the meshpoint closest to a zero. Therefore, we encountered no problems of numerical accuracy in determining the eigenvalues.

Once an eigenvalue is determined, the amplitudes A_I' , B_I' are obtained from (167), (168) then A_I , B_I from (163), (164). The amplitude C_0 of the radial wavefunction $R_0(r)$ in region 0

(see Eq. (34) is found from the continuity condition (48) and, finally, the overall normalisation constant \mathcal{N} from (52). The integral in Eq. (52) is done numerically.

We note that the numerical determination of the eigenvalues and eigenfunctions turned out to be extremely rapid. Thus it is conceivable that one uses these eigenfunctions (in principle completed by the scattering states) as basis functions for diagonalizing the additional polarization potentials studied in Sec. 3.

We note in passing that A'_I has in general a very small value which is difficult to obtain with sufficient accuracy from Eq. (167). It turned out that an accurate value of A'_I can be obtained by solving the equation (171) for A'_I at the value of the eigenvalue which had been determined before.

It is found that there are 3 classes of eigenfunctions: "external" or "class 1"-states which are predominantly localized in the vacuum outside of the insulator ($r > R_1$), "internal" or "class 2"-states which are mainly localized within the metallic core ($r < R_2$), and "class 3"-states which exhibit a non-negligible probability amplitude both in region 0 and region II. For a sufficiently large value of B , the probability for finding the electron in region I, i.e. within the insulator, turns out to be negligibly small. The spectrum of class 1-states resembles the Coulomb spectrum. On the other hand, the eigenvalues of class 2-states, in lowest approximation, are given by the eigenvalues of an infinite spherical square well of radius R_2 i.e. by the boundary condition $j_l(\kappa_{II}R_2) = 0$.

If $\kappa_{II}R_2 \gg 1$, the spherical Bessel function $j_l(\kappa_{II}R_2)$ can be approximated by

$$j_l(\kappa_{II}R_2) \approx \frac{1}{\kappa_{II}R_2} \cos \left[\kappa_{II}R_2 - \frac{l\pi}{2} - \frac{\pi}{4} \right]. \quad (178)$$

The zeros of this function together with (12) lead to the energy formula

$$E_{nl} = -V_{II} - \frac{Ze_0^2}{R_2} + \frac{\hbar^2\pi^2}{2MR_2^2} \left(\frac{3}{4} + n + \frac{l}{2} \right)^2, \quad (179)$$

where $n = 0, 1, \dots$ as well as l .

The spacing between neighbouring levels of given l or given n is

$$E_{n+1,l} - E_{nl} = \frac{\hbar^2\pi^2}{2MR_2^2} \left(\frac{5}{2} + 2n + 2l \right), \quad (180)$$

$$E_{n,l+1} - E_{n,l} = \frac{\hbar^2\pi^2}{2MR_2^2} \left(1 + n + \frac{l}{2} \right). \quad (181)$$

One should notice the completely different spacing of the eigenvalues of internally located electrons from the Coulomb dominated spacing of externally located electrons. Of course, if $\kappa_{II}R_2$ is not large compared to 1, the simple results (178) to (181) do not hold.

If it happens that, for given l , the energy of a predominantly externally and of a predominantly internally localized state come very close to each other, the corresponding eigenfunctions are not negligible in both the regions II and 0. We call eigenstates of this nature "class 3"-states. These states play an important role in the lifetime of the system and we shall come back to them in Subsec. 4.2.

In Fig. 3, we show the spectrum of eigenvalues ε for $l = 0$, $l = 1$, and $l = 10$ for a given set of parameters. We note that, apart from the dimensionless parameters defined in the text, lengths are given in Ångström (10^{-10} m) and energies in meV (10^{-3} eV).

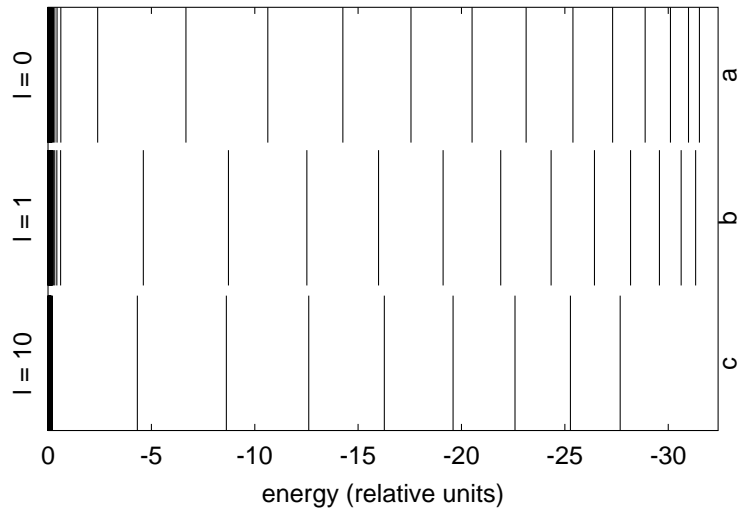


Figure 3: Comparison of the spectra of $l = 0$ states (Fig. 3a) and $l = 1$ states (Fig. 3b) and $l = 10$ states (Fig. 3c) for the following set of parameters: $Z = 1$, $R_1 = 28 \text{ \AA}$; $R_2 = 20 \text{ \AA}$; $V_{\text{II}} = 15950 \text{ meV}$; $b = 5.83$; $v_{\text{II}} = 31.031$, $R_0 = 0.271 \text{ \AA}$; $\varepsilon_{\text{min}} = 0.1$; $\varepsilon_{\text{max}} = 32.41$; energy mesh $\Delta\varepsilon = 0.0001$. Energy unit: $Ze_0^2/R_1 = 514 \text{ meV}$.

Given the energy unit $Ze_0^2/R_1 = 514 \text{ meV}$ in Fig. 3, the $|\varepsilon|$ -values belonging to externally located states must be smaller than 514 meV. The lowest-lying external state corresponds to the lowest line of the bunch of narrowly spaced lines at the top of the spectrum at $\varepsilon = 0,68$ or $E = -350 \text{ meV}$. Note that the energy difference between the first excited external s -state and the lowest external s -state is about 69,5 meV. This is also the order of magnitude of the average distance between low-lying external levels. Since the "room temperature" of 300° K corresponds to 26 meV, one may conclude that, at room temperature, for the parameter set chosen in Fig. 3, the externally bound electrons are predominantly in their lowest available states.

The spectrum of eigenvalues looks similarly for different fixed values of the angular momentum l . The fact that we show only the subsets of eigenvalues for given l -values in Fig. 3 should not lead to the erroneous impression that the levels of internally located electrons are so widely spaced that in general, no level of internal electrons is to be expected in the range of energies of external electrons. This is not so due to the fact that there are also the levels for $l \neq 0$. Consequently, there are generally "intruders" of internal levels in the spectrum of external ones and, consequently, there is in general also a limited number of "class 3-states" which, as we shall show, lead to rapid decay.

We should also notice in Fig. 3 that the distance between successive eigenvalues for given l increases with increasing eigenvalue, i.e. as $|\varepsilon| \rightarrow 0$. The reason for this trend is qualitatively seen from the formulae (180) and (181). For the parameter set chosen in Fig. 3, these approximate formulae are only valid for the high-lying levels.

In Fig. 4, we show the wavefunctions corresponding to internal s -states with 0, 1, and 8 radial nodes. It should be noted that even for the case of the highest one with 8 radial nodes at $|\varepsilon| = 17,96$, the localization within region II is perfect and the tails in region I are very tiny.

In Fig. 5, we present a comparison of external s -wavefunctions for radial node numbers $n = 0, 1$, and 5. Again one notices that the wavefunctions dive only weakly into region I and

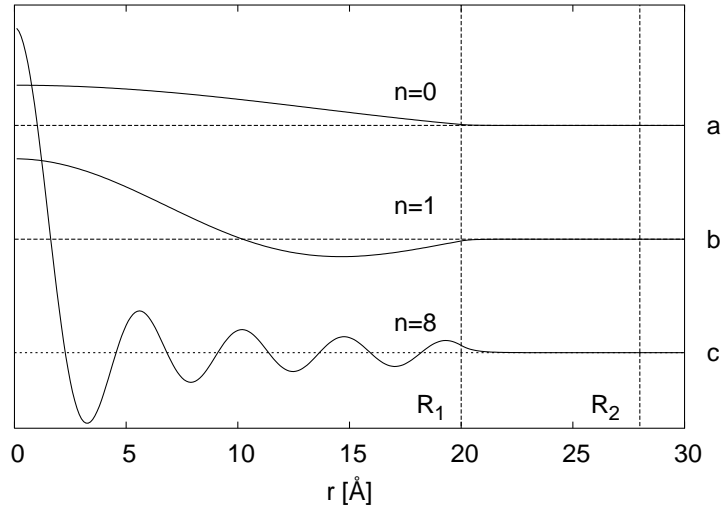


Figure 4: Internally located wavefunction (class 2-states) with radial node number $n = 0$ (Fig. 4a), $n = 1$ (Fig. 4b), and $n = 8$ (Fig. 4c). Orbital angular momentum $l = 0$. Energies (in units of $Ze_0^2/R_1 = 514.3 \text{ meV}$): $|\varepsilon(n = 0; l = 0)| = 32,235$; $|\varepsilon(n = 1; l = 0)| = 31,698$; $|\varepsilon(n = 8; l = 0)| = 17.963$. Choice of parameters as in Fig. 3.

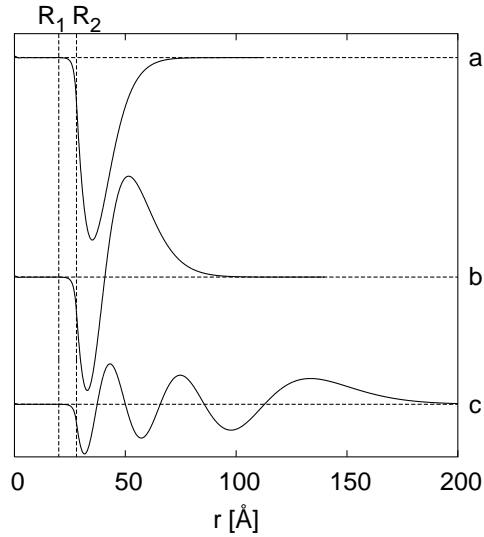


Figure 5: Externally located wavefunctions (class 1-states) with radial node number $n = 0$ (Fig. 5a), $n = 1$ (Fig. 5b) and $n = 5$ (Fig. 5c). Orbital angular momentum $l = 0$ energies (in units of $Ze_0^2/R_1 = 514.3 \text{ meV}$): $|\varepsilon(n = 0; l = 0)| = 0.63325$; $|\varepsilon(n = 1; l = 0)| = 0.44533$; $|\varepsilon(n = 5; l = 0)| = 0.18213$. Choice of parameters as in Fig. 3.

are completely negligible in region II. The energy difference ($E_{n=1,l=0} - E_{n=0,l=0}$) between the two lowest-lying external levels turns out to be 96 meV. The parameter set was chosen to be the same for the Figs. 3–5.

For the high-lying eigenenergy $E_{n=8,l=0} \approx -93,5$ meV the most external maximum of the wave function is seen to occur at $r \approx 130 \text{ \AA}$ whereas the wavefunction of the lowest external s -state with $n = 0$ becomes vanishingly small already at $r \approx 60 \text{ \AA}$. This strong dependence of the radial extension on the energy of the state is typical for a Coulomb-spectrum.

The class 1- and class 2-states are thus of very different nature. The eigenvalues of class 1-states must be above the potential energy ($-Ze_0^2/R_1$) on the surface S_1 of the insulator. Their spacing is much smaller than the one of class 2-states and tends to zero as the binding energy approaches zero. The lowering of the well-depth $-V_{\text{II}}^0$ by the potential produced by the positive surface charge on the metal surface S_2 and the screening effects in the insulator is given by $-[Ze_0^2/(\varepsilon_I R_2) + Ze_0^2(\varepsilon_I - 1)/(\varepsilon_I R_1)]$. This lowering of the Fermi energy E_F in the metal is larger than the minimal binding energy $-[Ze_0^2/R_1]$ of the lowest external electron by the amount

$$\Delta E := -\frac{Ze_0^2}{\varepsilon_I} \left[\frac{1}{R_2} + \frac{\varepsilon_I - 1}{R_1} \right] + \frac{Ze_0^2}{R_1} = -\frac{Ze_0^2}{\varepsilon_I} \left(\frac{1}{R_2} - \frac{1}{R_1} \right) \quad (182)$$

For the choice $R_1 = 28 \text{ \AA}$ and $R_2 = 20 \text{ \AA}$ and the charge number $Z = 1$, we have

$$\Delta E = -\frac{205,7 \text{ meV}}{\varepsilon_I}$$

i.e. a number between -20 and -200 meV depending on the dielectric constant ε_I of the insulator.

If there are unoccupied levels between the Fermi energy E_F and $(E_F + |\Delta E|)$, an electron in the lowest external state can decay into a lower-lying internal state.

4.2 Electromagnetic decay of external states

For the sake of simplicity, let us consider a system with one external electron and Z positive surplus charges. If the external electron is in some arbitrary externally located state it will first decay to the lowest-lying external state by a cascade of unhindered transitions. This lowest-lying external state is characterized by the angular momentum $l = 0$ and has no radial nodes ($n = 0$).

Subsequently, this lowest class 1-state will decay into lower-lying unoccupied internally located states (class 2-states). The strongest transitions are of multipolarity E1 and we only consider such dipole transitions. Even these most rapid transitions between a class 1 and a class 2 state are reduced in comparison with transitions between states of the same class due to the small overlap between externally and internally located wavefunctions.

The probability per time-unit for a dipole transition from the initial state ψ_i to the final state ψ_f is given by [8]

$$W_{12} = \frac{4\alpha c}{3} \frac{|E_1 - E_2|^3}{(\hbar c)^3} |\langle \psi_1 | \vec{r} | \psi_2 \rangle|^2, \quad (183)$$

where E_2 and E_1 denote the final and initial energy, resp., and $\alpha \equiv e_0^2/(\hbar c)$ is the fine structure constant.

The initial and final wavefunctions are

$$\psi_1(r, \vartheta, \varphi) = \tilde{R}_{l_1}(r, E_1) Y_{l_1 m_1}(\vartheta, \varphi), \quad (184)$$

$$\psi_2(r, \vartheta, \varphi) = \tilde{R}_{l_2}(r, E_2) Y_{l_2 m_2}(\vartheta, \varphi), \quad (185)$$

Table 2: The quantities W_z and W_{\pm} entering the dipole transition probability (see Eqs. (188), (189)).

	$l_1 - l_2 = 1$	$l_1 - l_2 = -1$
$m_2 = m_1 + 1$	$W_- = \left[\frac{(l_1 - m_1 - 1)(l_1 - m_1)}{(2l_1 + 1)(2l_1 - 1) \cdot 2} \right]^{\frac{1}{2}}$	$W_- = - \left[\frac{(l_1 + m_1 + 1)(l_1 + m_1 + 2)}{(2l_1 + 1)(2l_1 + 3) \cdot 2} \right]^{\frac{1}{2}}$
$m_2 = m_1$	$W_z = \left[\frac{(l_1 - m_1)(l_1 + m_1)}{(2l_1 + 1)(2l_1 - 1)} \right]^{\frac{1}{2}}$	$W_z = \left[\frac{(l_1 - m_1 + 1)(l_1 - m_1 + 2)}{(2l_1 + 1)(2l_1 + 3)} \right]^{\frac{1}{2}}$
$m_2 = m_1 - 1$	$W_+ = - \left[\frac{(l_1 + m_1)(l_1 + m_1 + 1)}{(2l_1 + 1)(2l_1 - 1) \cdot 2} \right]^{\frac{1}{2}}$	$W_+ = \left[\frac{(l_1 - m_1 + 1)(l_1 - m_1 + 2)}{(2l_1 + 1)(2l_1 + 3) \cdot 2} \right]^{\frac{1}{2}}$

where we leave away the spin-functions, and where \tilde{R}_{l_1} , \tilde{R}_{l_2} are the properly normalized radial functions (51). The matrix-element factorizes

$$\langle \psi_2 | \vec{r} | \psi_1 \rangle = \int_0^{\infty} dr \tilde{R}_{l_2}(r) r^3 \tilde{R}_{l_1}(r) \cdot \int d\Omega Y_{l_2 m_2}^* \vec{e}_r Y_{l_1 m_1} . \quad (186)$$

It is easily seen that the following relation holds:

$$\left[\int d\Omega Y_{l_1 m_1}^* \vec{e}_r Y_{l_2 m_2} \right]^2 = |W_+|^2 + |W_-|^2 + |W_z|^2 , \quad (187)$$

where the quantities W_{\pm} and W_z are defined by

$$W_{\pm} := \mp \sqrt{\frac{4\pi}{3}} \int d\Omega Y_{l_1 m_1}^* Y_{1, \pm 1} Y_{l_2 m_2} , \quad (188)$$

$$W_z := \sqrt{\frac{4\pi}{3}} \int d\Omega Y_{l_1 m_1}^* Y_{10} Y_{l_2 m_2} . \quad (189)$$

They are evaluated in terms of Clebsch-Gordan coefficients using the Wigner-Eckart theorem [9]:

$$W_{\pm} := \mp \sqrt{\frac{2l_2 + 1}{2l_1 + 1}} C(l_2 1 l_1, m_2, \pm 1, m_1) C(l_2 1 l_1 0 0) , \quad (190)$$

$$W_z := \sqrt{\frac{2l_2 + 1}{2l_1 + 1}} C(l_2 1 l_1 m_2 0 m_1) C(l_2 1 l_1 0 0) . \quad (191)$$

The non-vanishing values for W_{\pm} and W_z are presented in Table 2. The radial integral, i.e. the 1st factor in Eq. (186) is evaluated numerically.

We consider the case that the initial state is the lowest external state, i.e. a nodeless wavefunction with $l_1 = 0$. Thus, the final angular momentum l_2 is equal to 1.

The final magnetic moments m_2 may have the value $m_2 = -1, 0, +1$.

We are mainly interested in the lifetime τ of a "mesoscopic atom" which is the inverse of the total decay rate P :

$$\tau := \frac{1}{P} . \quad (192)$$

The total decay rate P is defined by summing the transition probabilities W_{12} over all the unoccupied final states ψ_2 which are connected with the initial state ψ_1 by a finite matrix

Table 3: Separation energy W_0 of an electron, Fermi-energy E_F^0 and well depth V_{II}^0 of uncharged metals (in meV).

	Be	Na	Al	Ca	Fe	Cs	Au
W_0	3920	2350	4250	2800	4310	1810	4300
E_F^0	14300	3240	11700	4690	11100	1590	5530
V_{II}^0	18220	5590	15950	7490	15410	3400	9830

Table 4: Lifetime τ as a function of the outer radius R_1 (\AA) for: $Z = 1$; $R_2 = 20 \text{ \AA}$; $B = 3000 \text{ meV}$; $V_{\text{II}}^0 = 15950 \text{ meV}$ (Al). Lifetimes in units: sec, minute (min), day (d), year (a).

R_1	26	28	30	32	34	36	38	40
τ	4.83 sec	52.9 sec	20.4 min	9.76 h	12.9 d	432 d	40.8 a	1431 a

element $\langle \psi_1 | \vec{r} | \psi_2 \rangle$:

$$P = \sum_2' W_{12} . \quad (193)$$

Considering only dipole transitions is, of course, an approximation which yields only a lower limit for the total transition rate and an upper limit for the lifetime.

The restriction of the sum in (193) to unoccupied internal electronic states is indicated by the prime '.

At temperature 0, a dipole transition starting from the initial external s -state can go into all the $l_2 = 1$ states the energy of which is between the Fermi energy E_F^0 and the energy E_1 of the initial state

$$E_F^0 < E_2 < E_1 .$$

At finite temperature, one has to weigh all the final states with the factor

$$\left[1 - \frac{1}{\exp\left(\frac{E_2 - \mu}{T}\right) + 1} \right] .$$

So far, we calculated the lifetime for the case $T = 0$ only.

In Table 3, we present the well depth V_{II}^0 , the separation energy W_0 , and the Fermi energy $E_F^0 = V_{\text{II}}^0 - W_0$ for a couple of metals. We note that these empirical parameters have been determined for materials with macroscopic size, not for mesoscopic clusters of such materials. Nevertheless, the parameters can be expected to be essentially correct also for mesoscopic systems.

Let us now come to the results we obtained for the lifetime as a function of the different parameters of the system. We studied separately the dependence of the lifetime τ on the parameters R_1 , B , Z , and R_2 , keeping always all but one parameter fixed.

Dependence of τ on R_1

Augmenting R_1 for fixed value of R_2 enlarges the width of the barrier and, consequently, decreases the amplitude which an externally located electron has in the inner region II. As

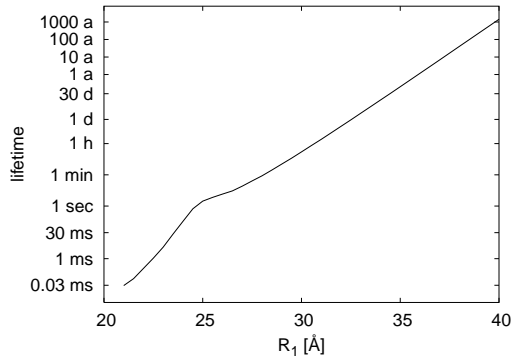


Figure 6: Lifetime in sec and logarithmic scale as a function of radius R_1 . Apart from R_1 , all the other parameters are chosen as in Fig. 3.

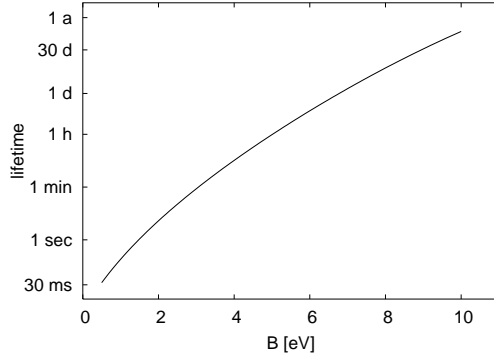


Figure 7: Lifetime τ in sec and logarithmic scale as a function of the barrier height B . Apart from B , all the other parameters are chosen as in Fig. 3.

the decay of a class 1-state into a class-2 state depends strongly on this tail, the transition probability must decrease and the lifetime must increase as a function of rising R_1 . The results presented in Table 4 support this expectation. The lifetime τ is found to rise roughly exponentially with $(R_1 - R_2)$. This is so because the amplitude of the tail in region II depends exponentially on $(R_1 - R_2)$ as one can see from WKB. The dependence of τ on R_1 is also shown in Fig. 6 in logarithmic scale.

Dependence of τ on the barrier height B

In Fig. 7, we show the dependence of the lifetime τ on the barrier height B in logarithmic scale. The lifetime increases as a function of rising B . The increase is somewhat smaller than exponential as can be expected from WKB.

Dependence of τ on R_2 and on Z

If one changes R_2 with all the other parameters fixed, one modifies predominantly the internally located class 2 states and the corresponding energies. As one can see from Fig. 8, the lifetime τ as a function of rising R_2 decreases on the average as one would expect from the fact that the thickness $(R_1 - R_2)$ of the surface layer decreases. However, beside the average decrease of the lifetime, one observes a kind of resonance structure: Within a change of R_2 by

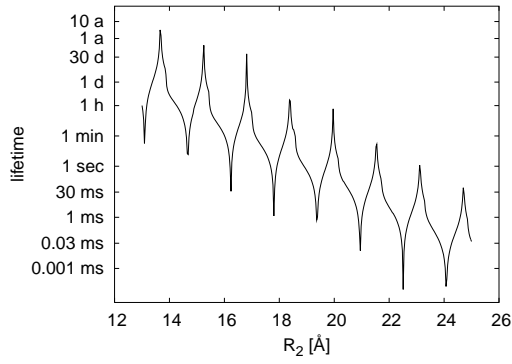


Figure 8: Lifetime τ in sec and logarithmic scale as a function of R_2 . Apart from R_2 , all the other parameters are chosen as in Fig. 3.

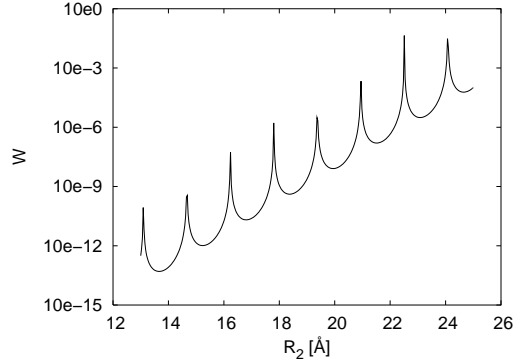


Figure 9: Probability (W) of lowest external electron to be found in the inner region II ($R < R_2$) as a function of R_2 . Apart from R_2 , all the other parameters are chosen as in Fig. 3.

1 Å, the lifetime τ can change by 10 orders of magnitude.

How can we understand these huge fluctuations of the lifetime?

In Fig. 9, we show the probability of an externally located electron to be found in the inner region II. This localization probability in region II, which is of crucial importance for the transition rate, is seen to show pronounced peaks at precisely those values of R_2 , where the lifetime has very small values as one can see by comparing Fig. 8 and Fig. 9. The large variations of the transition rate as a function of R_2 (and of Z) can be simply explained as follows:

As one changes R_2 (or Z), the eigenvalues of class 2-states move whereas the ones of class 1-states remain essentially the same. More specifically, the eigenvalues $E_{nl} = -|E_{nl}|$ of class-2 states are lowered, if the inner radius R_2 or the positive surplus charge Z is increased. Thereby, it happens regularly that a class 2-state which has the same angular momentum l as the decaying class 1-state, crosses the energy of this class 1-state. If one augments R_2 or Z on a sufficiently long scale, such crossings occur several times. Close to the crossing, the external class 1-state develops a non-negligible amplitude within region II and the class 2-state develops an appreciable amplitude in the external region 0. We call such mixed states "class 3-states". If the decaying class 1-state happens to have the nature of a class 3-state, its decay probability to lower-lying class 2-states is considerably enhanced as compared to the ordinary situation

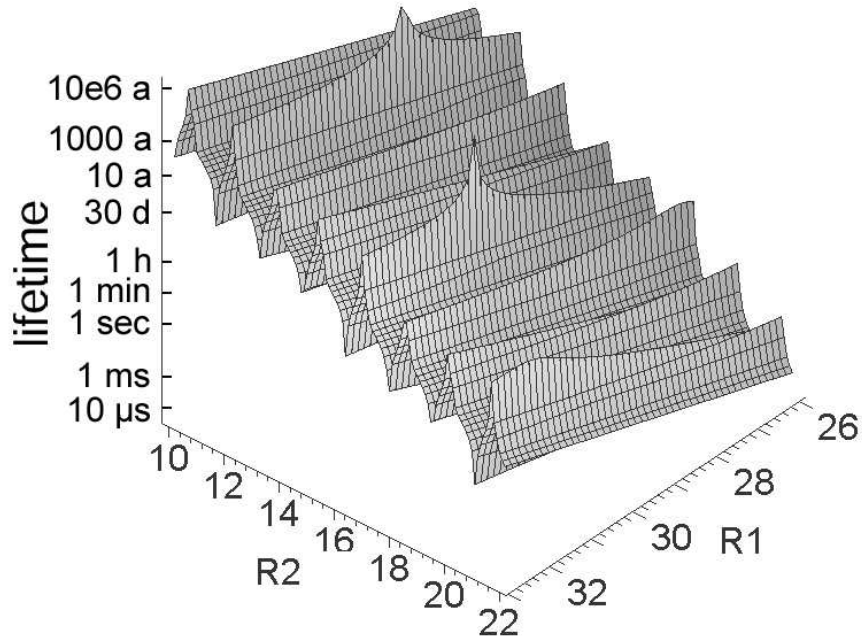


Figure 10: Lifetime τ (sec, log.scale) as a function of radius R_1 and R_2 (in \AA) in a 3-dimensional plot. Except for R_1 and R_2 , all the parameters are chosen as in Fig. 3.

where no class 2-state of the same angular momentum is available. We note in passing that this enhancement of the transition probability to lower-lying class 2-states does not only occur for dipole transitions but also for transitions of higher multipolarity. So far we have not yet calculated the transition rates of higher multipolarity, because they would only matter if the decaying external state is a class 3-state.

The phenomenon can be considered as an example of the mechanism which Landau and Zener had studied in famous papers [10]. This is demonstrated in Appendix.

In Fig. 10, the dependence of the lifetime τ on the radii R_1 and R_2 is shown in a 3-dimensional plot. Again one notices that the dependence of τ on R_1 is smooth whereas the one on R_2 contains "resonances".

In Fig. 11, the energy difference between the lowest-lying class 1 state and the closest lying class 2-state of the same angular momentum is shown. The plot supports the explanation of the resonance phenomenon in terms of a coupling between close-lying states.

In the numerical results presented in this section, the values B of the barrier in region I and the well depth V_{II} of the average potential in region II and the dielectric constant ϵ_1 were chosen arbitrarily, and not determined for given choices of the material.

5 Summary and Discussion

In this paper, we determined the quantum states and eigenenergies of an electron in the average potential produced by a positively charged metal cluster which is covered by an insulating surface layer. Because of the similarity of the externally localized electronic states with the

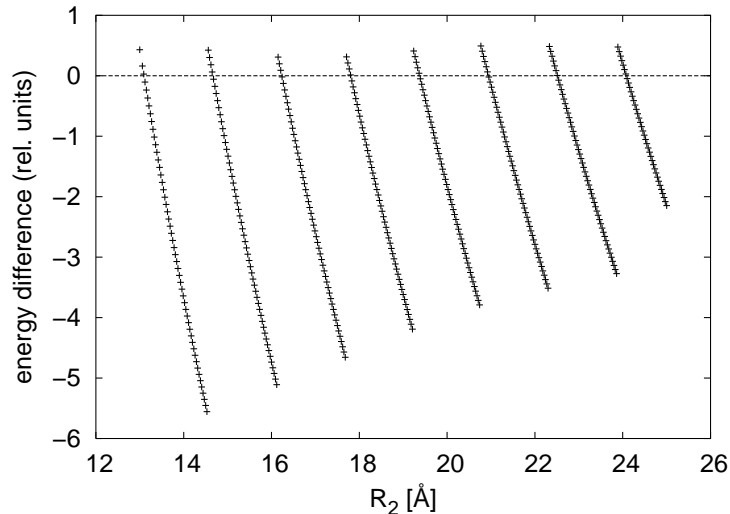


Figure 11: Energy difference between lowest-lying class 1-state and the closest lying class 2-state of the same angular momentum as a function of R_2 (\AA). Energies are given in units of $Ze_0^2/R_1 = 514.3$ meV. Except for R_2 , all the other parameters are chosen as in Fig. 3.

bound states of an electron in the Coulomb potential of an atom, we occasionally referred to the system as a "mesoscopic atom" or, in case of a non-zero total charge, as a "mesoscopic ion".

In particular, we investigated the electromagnetic decay of an externally located electron ("class 1-state") to a lower-lying unoccupied electronic state located within the metal ("class 2-state"). It turned out that the life-time depends sensitively on the radius R_2 of the metal core and on the number Z of positive surplus charges of the metal. In the model we studied, we found life-times varying between 10^{-10} s and years depending on the value of R_2 or of Z .

The value B of the barrier height was 3 eV in our calculations. The lifetime depends strongly on the value of this parameter and decreases for decreasing B .

The origin of the large fluctuations was found to be the appearance of states with non-negligible amplitudes both outside and inside of the insulating surface layer ("class 3-states"). The mechanism leading to these "class 3-states" is described in Appendix.

The wavefunctions and eigenenergies were calculated neglecting the polarization of the insulating surface layer by externally located electrons. The potential produced by these electronic polarization effects was determined in Sec. 3. It was shown that this additional potential matters mainly in the vicinity of the outer surface S_1 of the insulator and decreases exponentially outside of this surface. The polarization potential could be taken into account by diagonalizing the total Hamiltonian including the polarization potential in the basis of the wavefunctions determined in this paper.

Apart from this physical simplification of the problem we neglected the Coulomb potential produced by the positive surplus charge within the insulator. This approximation is justified whenever the change of the Coulomb potential within the insulating surface layer is much smaller than the barrier height B_0 . This condition was fulfilled in all the cases we studied numerically.

Let us now turn to the discussion of some open questions:

Is the model sufficiently realistic?

Certainly, our model should only be regarded as a first step which has to be improved in various respects.

The 1st improvement we already mentioned is to incorporate the additional potential between the external electron and the polarization cloud it produces in the insulator. The form of this electronic polarization potential was derived in Sec. 3.

A 2nd improvement would be to replace the constant potentials $-V_{\text{II}}^0$ in the metal and $+B_0$ in the insulator by periodic potentials defined by the crystal structure of these materials. Of course, this is much more complicated and, to our knowledge, it has rarely been done so far for mesoscopic systems. Furthermore, the crystal structure in mesoscopic aggregates is in general poorly known.

As a result, the electronic eigenvalues of the total system are expected to exhibit a band structure similarly to a macroscopic solid, the insulating surface layer being characterized by a completely filled valence band and an empty conduction band. The empty conduction band in the insulator can be at negative or at positive energy if the energy of the neutral system plus one electron at infinity is put equal to 0. Describing the average potential in the insulator by a positive barrier $B_0 > 0$ is only meaningful if the conduction band of the insulator is at positive energy.

As a further restrictive condition for our model to be a reasonable 1st approximation there should be no localized traps for an additional electron in the uncharged insulator. This implies that the individual atoms or molecules of the insulator should not have bound states with an additional electron as a monomer [11]. In general, bound states of an electron with a neutral atom or molecule do not exist for atoms or molecules with completely filled shells. Therefore, one should use insulators which exhibit this property. Presumably, Al_2O_3 fulfills this condition. Finally, we neglected effects of the electron-phonon coupling altogether. We presume that they tend to reduce the lifetime, but perhaps not drastically.

What were the physical motivations of this investigation

As long as one can only produce a limited number of "mesoscopic atoms", one could just investigate experimentally the effects which we studied in the present paper, especially the amusing strong dependence of the lifetime on the radius and the charge of the metallic core. Although we would be highly pleased by an experimental scrutiny of our predictions, still more exciting open questions could be asked, if it were possible to produce longlived systems of the kind we presented in this paper, and in large quantities. In this case, one would have access to the study of molecules formed from mesoscopic atoms and to condensed matter consisting of mesoscopic atoms as building blocks.

The presence of externally localized electrons would represent a fundamental difference from the case of a condensed system of uncharged mesoscopic clusters. On the one hand, one may expect that, in a condensed matter phase of mesoscopic atoms, the weakly bound external electrons would partly dissociate from their mother atoms and move freely in the average field produced by the charged insulated cores. We would thus surmise that such a system would be a (good) conductor. On the other hand, the fact that the building blocks of such a condensed matter carry charge, will have a profound influence on the equilibrium state of the material. Probably, its density is lower than for uncharged constituents, where the cohesive forces are of van der Waals type and, consequently, of much shorter range.

How far are such dreams from reality?

There are evidently two fundamental obstacles to overcome, a theoretical one and an experimental one.

The theoretical problem is the stability of the charged and insulated single system, and the experimental one is the production of a large number (10^{23}) of such systems.

As we learnt from this paper, a mesoscopic system of the kind we investigated can only be stable in a strict sense, if there is no empty internally located electronic state below the energy of the lowest externally located state which is at an energy slightly above $-Ze_0^2/R_1$.

The positive surplus charge Ze_0 on the surface S_2 of the metal leads to a decrease of the well-depth $V_{\text{II}}^0 \rightarrow V_{\text{II}}$ as we have shown in Sec. 3:

$$V_{\text{II}} = V_{\text{II}}^0 - \frac{Ze_0^2}{\varepsilon_1} \left(\frac{1}{R_2} + \frac{\varepsilon_1 - 1}{R_1} \right). \quad (194)$$

If, for the uncharged metal, the Fermi level is at the energy $E_F^0 - V_{\text{II}}^0$ (with $V_{\text{II}}^0, E_F^0 > 0$), it lies at the modified energy

$$E_F^0 - V_{\text{II}} = E_F^0 - V_{\text{II}}^0 + \frac{Ze_0^2}{\varepsilon_1} \left(\frac{1}{R_2} + \frac{\varepsilon_1 - 1}{R_1} \right) \quad (195)$$

in the charged metal.

So the condition for strict stability is that there is no level of an internally located electron between $E_F^0 - V_{\text{II}} < 0$ and $-Ze_0^2/R_1$. As the separation energy $W_0 > 0$ of an electron from the uncharged metal and the Fermi energy E_F^0 are related to V_{II}^0 by

$$V_{\text{II}}^0 = E_F^0 + W_0, \quad (196)$$

we can state that strict stability is achieved whenever there is no level between the energies $-\{W_0 - Ze_0^2/\varepsilon_1 \cdot [1/R_2 + (\varepsilon_1 - 1)/R_1]\}$ and $-Ze_0^2/R_1$. This means that, metal with small W_0 is favourable for stability.

In an ordinary metal, the separation energy W_0 is of the order of a couple of eV (examples: $W_0(\text{Al}) = 4,28$ eV; $W_0(\text{Ag}) = 4,26$ eV). In the case of a radius $R_2 = 20$ Å of the metal core, the distance between neighbouring electronic levels is of the order of 100 meV. This means that in the case we chose for our numerical investigations, there are many unoccupied levels below the energy of the lowest external electron. However, if we consider a system with an inner radius $R_2 \approx 4$ Å, the spacing of internally located electron levels of given l approaches already 1 eV. It is therefore conceivable that one might succeed to model a strictly stable „mesoscopic atom”.

A further trick to widen the spectrum of internally localized electrons would be to replace the metallic sphere with radius R_2 by a metallic bubble of outer radius R_2 and a thickness of 1 Å to 2 Å. In this case the levels differing by the number of radial nodes would have a much larger spacing.

Can such a system be made experimentally?

This is perhaps possible, if one replaces the charged metal layer by a (charged) fullerene C_{60} , which has a radius of about 3,5 Å. The separation energy W_0 of an electron from graphite is known to be $W_0 = 3,8$ eV. We surmise that the separation energy from the fullerene is about the same. Of course, it would no longer be justified to describe free electrons in the fullerene as moving in a simple square well perpendicular to the sphere S_2 . But the spacing of electronic levels is expected to be in the order of eV.

Finally, one is not limited to the spherical geometry. We may also envisage to consider charged nanotubes consisting of a cylindrical surface crystal of C -atoms covered by an insulating

surface layer. The charge could in this case be generated by applying an external voltage to the ends of the nanotubes. As there is a lot of activity spent on nanotubes presently, we hope that one could succeed to produce small macroscopic amounts of insulated charged nanotubes in a not too far future. Of course, the problem of the stability of externally localized electrons with respect to electromagnetic decay would be similar for nanotubes as for the case of the system we investigated. So we hope that our investigation stimulates the interest of the experts in the field of mesoscopic physics.

Acknowledgement:

Klaus Dietrich gratefully acknowledges the hospitality and support on the occasion of his stay at the Theoretical Physics Institute of the UMCS in April 2003. Krzysztof Pomorski is indebted to the Physics Department of the Technical University of Munich for granting of the honorarium of a visiting professor position in February 2002.

Appendix

Landau-Zener Model for explaining the appearance of class 3-states

Let us consider the simplified potential

$$\widehat{V}(r) = -V_{\text{II}}\theta_0(R_2 - r) + B\theta_0(R_1 - r)\theta_0(r - R_2) - \frac{Ze_0^2}{r}\theta_0(r - R_1) . \quad (197)$$

We decompose this potential as follows

$$\widehat{V}(r) = \widetilde{V}_1(r) + \widetilde{V}_2(r) , \quad (198)$$

$$\widehat{V}_1(r) = \theta_0(r - R_1) \left[-B - \frac{Ze_0^2}{r} \right] , \quad (199)$$

$$\widehat{V}_2(r) = -V_{\text{II}}\theta_0(R_2 - r) + B\theta_0(r - R_2) \quad (200)$$

and define the two Hamiltonians

$$\widehat{H}_{1(2)} := \widehat{T} + \widehat{V}_{1(2)}(r) , \quad (201)$$

where \widehat{T} is the kinetic energy operator of radial motion

$$\widehat{T} = -\frac{\hbar^2}{2M} \left(\frac{d^2}{dr^2} + \frac{2}{r} \frac{d}{dr} - \frac{l(l+1)}{r^2} \right) . \quad (202)$$

The eigenstates $\varphi_\nu^{(1)}$, $\varphi_\nu^{(2)}$ of the Hamiltonians (201)

$$\widehat{H}_1\varphi_\nu^{(1)}(r) = E_\nu^{(1)}\varphi_\nu^{(1)} , \quad (203)$$

$$\widehat{H}_2\varphi_\nu^{(2)}(r) = E_\nu^{(2)}\varphi_\nu^{(2)} \quad (204)$$

form a non-orthogonal set of basis functions.

We consider an eigenstate ψ of the Hamiltonian \widehat{H} with eigenenergy E

$$\widehat{H} := \widehat{T} + \widehat{V}(r) , \quad (205)$$

$$\widehat{H}\psi = E\psi \quad (206)$$

for the special case that the angular momentum l is the same for all the states and that two specific eigenenergies $E_\nu^{(1)}$ and $E_\nu^{(2)}$ are very close to the energy E in (206).

Then, we may expect that the expansion of ψ in terms of the basis states $\varphi_\nu^{(1)}$ and $\varphi_\nu^{(2)}$ may be limited to the two states with the energies $E_\nu^{(1)}$, $E_\nu^{(2)}$ very close to E_ν :

$$|\psi\rangle = A_\nu|\varphi_\nu^{(1)}\rangle + B_\nu|\varphi_\nu^{(2)}\rangle . \quad (207)$$

In principle, we would have to sum over all eigenstates $\varphi_\nu^{(1)}$ and $\varphi_\nu^{(2)}$ on the righthand side of (207), but of all the expansion coefficients A_ν , B_ν only the ones corresponding to the energies $E_\nu^{(1)}$, $E_\nu^{(2)}$ closest to E are expected to be large and all the others to be much smaller.

Henceforth, we leave away the subscript ν for simplifying the notation. It is convenient to introduce the dual basis states $\tilde{\varphi}^{(1)}$, $\tilde{\varphi}^{(2)}$ defined by the orthogonality conditions

$$\langle \tilde{\varphi}^{(i)} | \varphi^{(j)} \rangle = \delta_{ij} , \quad (208)$$

where i and j can be 1 or 2. $\tilde{\varphi}^{(1)}$ and $\tilde{\varphi}^{(2)}$ can be obtained by diagonalizing the inverse of the overlap matrix

$$M^{(ij)} = \langle \varphi^{(i)} | \varphi^{(j)} \rangle . \quad (209)$$

It is easily seen that the Schrödinger Eq. (206) together with the assumption (207) leads to the two coupled linear equations

$$\begin{pmatrix} (E^{(1)} - E + V_2^{11}) & V_1^{12} \\ V_2^{21} & (E^{(2)} - E + V_1^{22}) \end{pmatrix} \begin{pmatrix} A \\ B \end{pmatrix} = 0 , \quad (210)$$

where the matrix elements are defined as follows:

$$V_{1,2}^{ij} := \langle \tilde{\varphi}^{(i)} | V_{1,2} | \varphi^{(j)} \rangle . \quad (211)$$

Introducing the abbreviations

$$\tilde{E}^{(1)} := E^{(1)} + V_2^{11} , \quad (212)$$

$$\tilde{E}^{(2)} := E^{(2)} + V_1^{22} \quad (213)$$

the solutions E_{\pm} of the eigenvalue equation

$$(\tilde{E}^{(1)} - E)(\tilde{E}^{(2)} - E) - V_1^{12} \cdot V_2^{21} = 0 \quad (214)$$

are given by

$$E_{\pm} = \frac{\tilde{E}^{(1)} + \tilde{E}^{(2)}}{2} \pm \frac{1}{2} \sqrt{(\tilde{E}^{(1)} - \tilde{E}^{(2)})^2 + 4V_1^{12}V_2^{21}} . \quad (215)$$

Writing the two states $|\psi\rangle$ in the form

$$|\psi_{\pm}\rangle = A_{\pm} \cdot \{ |\varphi^{(1)}\rangle \pm \lambda_{\pm} |\varphi^{(2)}\rangle \} , \quad (216)$$

where

$$\lambda_{\pm} := \frac{B_{\pm}}{A_{\pm}} , \quad (217)$$

one obtains λ from the Eq. (210) and the amplitudes A_{\pm} from the normalisation of $|\psi_{\pm}\rangle$.

The physically interesting quantities are the probabilities $W_{+}^{(1,2)}$ and $W_{-}^{(1,2)}$ to find the system described by $|\psi_{\pm}\rangle$ in the substate $\varphi^{(1)}$ or $\varphi^{(2)}$. These probabilities are given by the mean-values of the projection operators

$$\hat{P}_{(1,2)} := |\varphi^{(1,2)}\rangle \langle \tilde{\varphi}^{(1,2)}| . \quad (218)$$

It is easily seen that the probabilities are given by the following equations

$$W_{+}^{(1)} = \langle \psi_{+} | \hat{P}_{(1)} | \psi_{+} \rangle = \frac{1 + \lambda_{+} M^{12}}{1 + 2\lambda_{+} M^{12} + \lambda_{+}^2} , \quad (219)$$

$$W_{+}^{(2)} = \langle \psi_{+} | \hat{P}_{(2)} | \psi_{+} \rangle = \frac{\lambda_{+} (\lambda_{+} + M^{12})}{1 + 2\lambda_{+} M^{12} + \lambda_{+}^2} , \quad (220)$$

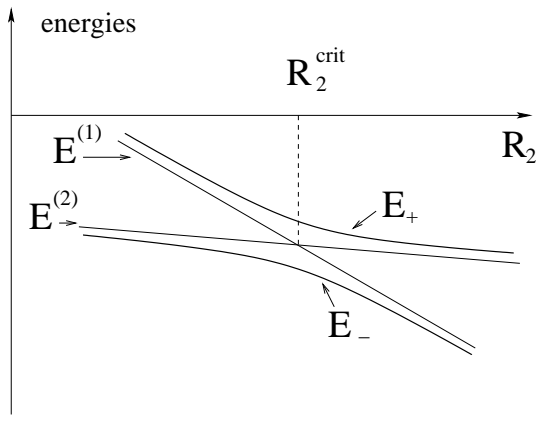


Figure 12: Schematic plot of the Landau-Zener crossing of an external and an internal energy $E^{(1,2)}$ yielding the class 3-state energies E_{\pm} .

$$W_-^{(1)} = \langle \psi_- | \hat{P}_{(1)} | \psi_- \rangle = \frac{1 - \lambda_- M^{12}}{1 - 2\lambda_- M^{12} + \lambda_-^2}, \quad (221)$$

$$W_-^{(2)} = \langle \psi_- | \hat{P}_{(2)} | \psi_- \rangle = \frac{\lambda_- (\lambda_- - M^{12})}{1 - 2\lambda_- M^{12} + \lambda_-^2}, \quad (222)$$

where M^{12} is the overlap of the two basis states

$$M^{12} = \langle \varphi^{(1)} | \varphi^{(2)} \rangle \quad (223)$$

and the quantities λ_{\pm} by

$$\lambda_{\pm} = \frac{1}{2V^{12}} \left\{ -\Delta E^{(1,2)} \pm \sqrt{(\Delta E^{(1,2)})^2 + 4V_1^{12}V_2^{21}} \right\}, \quad (224)$$

where

$$\Delta E := E^{(1)} - E^{(2)}. \quad (225)$$

It is seen that for

$$|\Delta E|^2 \gg 4|V_1^{12} \cdot V_2^{21}|, \quad (226)$$

i.e. far away from the crossing of the energies $E^{(1)}$ and $E^{(2)}$, one of the ratios λ_{\pm} is much larger than the other.

For $\Delta E > 0$ one finds

$$\lambda_+ \approx \frac{V_2^{21}}{\Delta E}, \quad (227)$$

$$\lambda_- \approx - \left[\frac{\Delta E}{V_1^{12}} + \frac{V_2^{21}}{\Delta E} \right] \quad (228)$$

and for $\Delta E < 0$ the reversed result

$$\lambda_+ \approx \frac{\Delta E}{V_1^{12}} + \frac{V_2^{21}}{|\Delta E|}, \quad (229)$$

$$\lambda_- \approx - \frac{V_2^{21}}{|\Delta E|}. \quad (230)$$

This shows that a predominantly externally localized state turns into a predominantly internally localized one as the energies $E^{(1)}$ and $E^{(2)}$ cross as a function of R_2 or Z . The coupled true states ψ_{\pm} are thus seen to change their nature as a result of the crossing of the energies $E^{(1)}$, $E^{(2)}$ of a class 1 and a class 2 state. Close to the crossing point the states ψ_{\pm} are seen to be "delocalized", containing comparable contributions of the two basis states $\varphi^{(1,2)}$.

This is in essence a Landau-Zener crossing. In Fig. 12 we show a schematic picture of the energies $E^{(1)}$, $E^{(2)}$, E_+ , and E_- as a function of the parameter R_2 or Z .

References

- [1] W. D. Knight, K. Clemenger, W. A. de Heer, W. A. Saunders, M. Y. Chou, M. L. Cohen: Phys. Rev. Lett. **52**, (1984) 2141; W. D. Knight, W. A. de Heer, K. Clemenger, W. A. Saunders: Solid State Commun. **53**, (1985) 44; Hellmut Haberland (ed): "Clusters of Atoms and Molecules", vol. 1 and 2, Springer Verlag, 1994.
- [2] S. Frank, N. Malinowski, F. Tast, M. Heinebrodt, I.M.L. Billas, T.P. Martin: Z. Phys. **D40**, (1997) 250; M. Springborg, S. Satpathy, N. Malinowski, T.P. Martin, U. Zimmermann: Phys. Rev. Lett. **77**, (1996) 1127; H. Kuzmany, J. Fink, M. Mehring, S. Roth (eds): "Electronic Properties of Fullerenes", Springer-Verlag, 1993.
- [3] M. Brack: Rev. Mod. Phys. **65**, 677 (1993).
- [4] W. A. de Heer, Rev. Mod. Phys. **65**, 611 (1993).
- [5] M. Abramowitz and J.A. Stegun (eds): "Handbook of Mathematical Functions", Nat. Bureau of Standards, Applied Mathematics, Series 55, issued June 1964.
- [6] A. Erdelyi, "Higher Transcendental Functions", McGraw-Hill, 1953.
- [7] J.D. Jackson: "Classical Electrodynamics", John Wiley, 1967.
- [8] B.H. Bransden and C.J. Joachain, "Physics of Atoms and Molecules", Longman Group Limited, 1983.
- [9] M.E. Rose, "Elementary Theory of Angular Momentum", New York: Dover, 1995
- [10] L.D. Landau, Phys. Z. Sov. **2** (1932) 46; C. Zener, Proc. Roy. Soc. (London) **A137** (1932) 696.
- [11] H. Haberland and K.H. Bowen: "Solvated Electron Clusters", Chapt. 2.5 in "Cluster of Atoms and Molecules II", vol. 56 of the Springer Series in Chemical Physics, 1994.